

Université de Montréal

Novel electrochemical aptamer-based sensing mechanism inspired by selection strategies

Par

Tatiana Lyalina

Département, de Chimie, Faculté des Arts et Sciences

Mémoire présenté en vue de l'obtention du grade de M.Sc.

en chimie

Janvier 2023

© Tatiana Lyalina, 2023

Université de Montréal

Département de Chimie, Faculté des Arts et Sciences

Ce mémoire intitulé

Titre du mémoire

Novel electrochemical aptamer-based sensing mechanism inspired by selection strategies

Présenté par

Tatiana Lyalina

A été évalué par un jury composé des personnes suivantes

Antonella Badia

Président-rapporteur

Alexis Vallée-Bélisle

Directeur de recherche

Joelle Pelletier

Membre du jury

Résumé

Des millions de patients souffrant d'insuffisance cardiaque bénéficieraient d'analyses sanguines hebdomadaires pour surveiller l'évolution de leur état de santé comme c'est le cas avec les personnes atteintes du diabète. Cependant, il n'existe pas de technologies d'analyses sanguines rapides et efficaces pour détecter des marqueurs d'insuffisance cardiaque, telle que la créatinine, la NT-proBNP et la troponine I par exemple. La possibilité pour les patients de surveiller leurs taux de créatinine régulièrement, du confort de chez soi, améliorerait largement leur qualité de vie ainsi que leur taux de survie. En suivant leur taux de créatinine, le patient pourrait prédire des signes d'insuffisance cardiaque, et ainsi faire ajuster leur plan de traitement en conséquence. Pour y arriver, les biocapteurs électrochimiques, dont un exemple est le glucomètre, représentent une classe prometteuse de dispositifs d'analyse sanguine puisqu'ils sont faciles à utiliser, rapides, peu coûteux, sensibles, stables et potentiellement universels. Les biocapteurs électrochimiques à base d'ADN pourraient potentiellement être adaptés en biocapteur de créatinine, par l'entremise d'aptamères. Le but de cette recherche est de développer un nouveau mécanisme de détection universel et efficace pouvant être adapté directement à partir des stratégies de sélection des aptamères. Pour ce faire, nous avons identifié et caractérisé un élément de biorecognition sélectif pour la créatinine. Ensuite, nous avons conçu une nouvelle stratégie de détection et nous avons validé cette nouvelle stratégie par spectroscopie de fluorescence avant de l'adapter pour une détection électrochimique. Par la suite, nous avons optimisé les performances du biocapteur en modulant des paramètres analytiques tels que sa gamme linéaire et son gain de signal, tout en validant ses performances dans une matrice complexe comme le sérum. Les résultats de cette recherche suggèrent que la stratégie de conception du nouveau biocapteur électrochimique à base d'aptamère est prometteuse pour la détection efficace de biomarqueurs sanguins. Ce type de mécanisme pourrait être facilement adapté pour détecter d'autres molécules cliniquement pertinentes en modifiant simplement la stratégie de sélection de l'aptamère.

Mots-clés : biocapteur, capteur électrochimique, aptamère, créatinine, SELEX, électrochimie, sérum, sang.

Abstract

Millions of patients suffering from heart failure would greatly benefit from weekly blood analysis to help them manage their disease state like patients suffering from diabetes. However, no simple blood monitoring technologies detecting heart failure biomarkers, such as creatinine, NT-proBNP, and troponin I, are available. The ability to determine and regularly monitor the creatinine level in the home setting would greatly improve the patient's quality of life and survival rate. Knowing the concentration of creatinine help to predict heart failure and to revise the treatment plan if the concentration of creatinine is abnormal. To achieve this, electrochemical sensors, like a glucometer, represent a promising class of blood analysis devices due to their ease of use, fast response, low cost, inherent sensitivity and stability, and potential universality. More specifically, DNA-based electrochemical biosensors could potentially be adapted into a creatinine sensor by using aptamers specific to a biomarker. To achieve this goal, we identified a selective biorecognition element for creatinine detection and characterized it. We also designed a novel sensing aptamer-based strategy and validated this strategy by fluorescent spectroscopy before transposing it into the electrochemical format. We then optimized the performance of the sensor by tuning its signal gain and characterizing the dynamic range while also validating its performance in serum. The results of this work suggest that the electrochemical aptamer-based strategy represents a promising sensing mechanism. We believe this mechanism could be easily adapted to detect other clinically relevant molecules by simply relying on the aptamer's selection strategy.

Keywords : Biosensor, electrochemical sensor, aptamer, creatinine, SELEX, electrochemistry, serum, whole blood.

Table of Contents

Résumé.....	3
Abstract.....	5
Table of Contents.....	6
List of Tables.....	9
List of Figures.....	10
List of abbreviations.....	12
Acknowledgements.....	14
Chapter 1 – Introduction.....	15
1. Monitoring Heart Failure.....	15
1.1. Creatinine: an important biomarker to assess renal function and predict heart problems.....	17
1.2. Current state-of-the-art detection of creatinine.....	20
1.2.1. Chemical method based on Jaffe’s reaction for detection of creatinine.....	20
1.2.2. Enzymatic strategies for the detection of creatinine.....	21
1.3. Biosensors as promising diagnostic devices.....	23
1.3.1. What is a biosensor?.....	23
1.3.2. Electrochemical DNA-based sensors.....	26
1.3.2.1. Background.....	26
1.3.2.2. E-DNA sensor.....	26
1.3.2.3. Electrochemical Aptamer-based sensors (AB-sensors).....	27
1.3.2.4. Kinetically programmed aptamer-based sensors.....	29
1.3.3. Novel aptamer-based signalling mechanism based on selection strategies.....	31

1.3.3.1.	Conventional aptamer selection strategies	31
1.3.3.2.	A capture-SELEX strategy	33
1.4.	Aim and thesis structure	37
Chapter 2 – Methodologies for the development of new electrochemical aptamer-based sensors		39
2.	Identifying a selective biorecognition element.....	41
2.1.	Analyzing DNA structure	41
2.1.1.	Measuring binding affinities using Isothermal titration calorimetry (ITC)	41
2.2.	Engineering a biosensing strategy.....	45
2.3.	Design and Synthesis of DNA strands	47
2.3.1.	Sequences of DNA-based sensor	47
2.3.2.	Synthesis of all designed strands	49
2.3.3.	Purification of DNA strands by Reverse Phase Cartridge.....	49
2.3.4.	Purification of labelled DNA strands by HPLC.....	49
2.3.5.	Quantification of DNA strands	50
2.4.	Fluorescent experiments.....	50
2.5.	Electrochemical sensor	51
2.5.1.	Electrode system	51
2.5.2.	DNA Immobilization onto the gold electrode surface	52
2.5.3.	Redox element	54
2.5.4.	Square wave voltammetry	55
2.5.5.	Optimal frequency for electron transfer.....	57
2.5.6.	Calculation of signal enhancement (signal gain).....	58
2.6.	Sensor characterization.....	58

2.7. Sensor validation in serum	59
Chapter 3 – Results and Discussion.....	60
3.1. Characterization of the creatinine aptamer.....	60
3.1.1. Characterization of the aptamer binding affinity	61
3.1.2. Attempt at designing a shorter creatinine aptamer	63
3.2. Engineering signalling mechanisms	65
3.2.1. Classic electrochemical aptamer-based assays.....	65
3.2.1.1. One-component assay	65
3.2.1.2. Three-component assay.....	65
3.2.2. Signalling strategies based on SELEX.....	67
3.2.2.1. Validating the signalling mechanism based on the selection strategy using fluorescence	67
3.2.3. Adapting the signalling mechanism into an electrochemical format	69
3.2.3.1. Design and validation	69
3.2.3.2. Optimizing the sigDNA:aptamer ratio.....	70
3.2.3.3. Other strategies to improve a signal gain	72
3.2.3.4. Determinating the dynamic range of the sensor	73
3.2.3.5. Detecting creatinine in serum.....	74
3.3. Potential universality of the SELEX-based sensing strategy	77
Chapter 4 – Conclusions and Outlook.....	79
References.....	82

List of Tables

Table 1.	2021 Statistics of the Heart and Stroke Foundation of Canada.....	15
Table 2.	Comparison of the point-of-care devices based on enzymatic reactions coupled with the electrochemical reader.....	22
Table 3.	Sequences of designed DNA strands.....	47

List of Figures

Figure 1.	Biosynthesis of creatine.	18
Figure 2.	Jaffe's reaction.	20
Figure 3.	Examples of three main enzymatic reactions to detect creatinine.	21
Figure 4.	The scheme represents the main components of the biosensor	23
Figure 5.	Commercially available biosensors.	24
Figure 6.	One component E-DNA sensor based on DNA hybridization.	27
Figure 7.	E-AB sensors based on binding-induced conformational changes.	28
Figure 8.	Representation of the new kinetically programmed strategy.	30
Figure 9.	General scheme of SELEX (Systematic Evolution of Ligands by Exponential enrichment) process with main steps.	32
Figure 10.	Example of a capture-SELEX procedure optimized by M. Stojanovic. ⁷⁰	34
Figure 11.	Capture-SELEX strategies enable easy adaptation into a fluorescent sensor.	36
Figure 12.	Designing an aptamer-based signalling mechanism based on its selection strategy (capture-SELEX)..	37
Figure 13.	Overview of the methodology to create a new sensing strategy based on the capture-SELEX selection strategy..	40
Figure 14.	Overview of Isothermal Titration Calorimetry.	42
Figure 15.	The examples of simulated curves at different c-values using the same ligand and titrant.....	43
Figure 16.	The biosensing strategy based on the capture-SELEX strategy.	45
Figure 17.	The screen-printed electrode 'Phase Zero Sensors'.	51
Figure 18.	Schematic design of the capDNA and its immobilization onto the gold electrode surface.....	53
Figure 19.	Redox element – methylene blue.	54
Figure 20.	Square wave voltammetry overview.	55
Figure 21.	Lovric Graph shows the dependence of cumulative charge and frequency.....	57
Figure 22.	Characterization of the creatinine aptamer.....	61

Figure 23.	ITC characterization of the creatinine aptamer.	62
Figure 24.	Reducing the length of the aptamer reduces its affinity for creatinine.	64
Figure 25.	Adapting the creatinine aptamers into a “three-component” strategy failed	66
Figure 26.	The importance of the sigDNA location in fluorescent assays..	68
Figure 27.	Electrochemical adaptation of the signalling mechanism.	70
Figure 28.	Optimizing the signal gain by exploring different sigDNA:aptamer ratios (from 1:1 to 1:4).....	71
Figure 29.	Increasing the hybridization length and affinity of the sigDNA for the aptamer reduces background signal and improves signal gain.	73
Figure 30.	Binding curve and dynamic range of the electrochemical creatinine sensor.....	74
Figure 31.	Creatinine detection directly in serum.	76
Figure 32.	Developing a moxifloxacin sensor using a SELEX-based signalling mechanism. ...	78

List of abbreviations

BHQ-1 : Black Hole Quencher – 1

CAD : Canadian dollar

CapDNA : Capturing DNA

DNA : Deoxyribonucleic acid

E - AB : Electrochemical aptamer-based sensors

E - DNA : Electrochemical DNA-based sensors

FAM : 6-Carboxyfluorescein

GFR : Glomerular filtration rate

ITC : Isothermal titration calorimetry

K_d : Dissociation constant

MCH : 6-Mercapto-1-hexanol

nt : Nucleotide

RNA : Ribonucleic acid

SELEX : Systematic Evolution of Ligands by Exponential Enrichment

SigDNA : Signalling DNA

WC : Watson Crick base pairs

Science and everyday life cannot and should not be separated. Science, for me, gives a partial explanation of life. In so far as it goes, it is based on fact, experience and experiment.

Rosalind Franklin

Acknowledgements

I would like to thank my committee members Prof. Joelle Pelletier, Prof. Antonella Badia, who have provided valuable comments, insights, directions, and many discussions.

I would like to thank my supervisor, Prof. Alexis Vallée-Bélisle, for giving the opportunity and accepting me into his research group. I am also grateful for providing guidance and spending dozens of hours of his time.

I would like to acknowledge the lab members of AVB lab. I greatly enjoyed working with Dominic Lauzon, Guichi Zhu, Xiaomeng Wang, Arnaud Desrosiers, Simon Diallo Blais, Yasmine Nicole, Nagarjun Narayana Swamy, Liliana Perdo and Scott Harroun. I could not have asked for better friends and colleagues, and I truly hope we will still keep in touch.

During my time as a PhD candidate and then as a Master's student at Université de Montréal, it was my privilege and pleasure to interact with faculty staff as well as with TransMedTech and PROMOTE NSERC scholars and coordinators.

I would have had a tough time getting through this degree without my friends, colleagues, and mentors. Last but not least, I would like to thank my family, who supports me during my studies and continuously believes in me. Without my family, none of this would have been possible.

Chapter 1 – Introduction

Heart failure tops the list of diseases causing death in developed countries, such as the United States and Canada, costing over \$30 billion yearly.^{1, 2} By 2030, it is estimated that ~2-3 % of North America's population (10 million people) will be prone to developing heart failure. In Canada, heart failure has already reached 2 % of the population (Table 1), and the numbers are steadily increasing. According to a recent survey, one in three Canadians is affected by heart failure; they either suffer from heart failure themselves or their relatives and friends have been affected by it. It is the fastest uncontrollable spreading cardiovascular condition.³

Table 1. 2021 Statistics of the Heart and Stroke Foundation of Canada. Experts predict an increase in the people affected or diagnosed with heart failure.

Population in Canada	37 000 000
Living with heart failure	750 000
Diagnosed with an incurable condition	100

The main challenge confronting heart failure patients is that nearly 1 in 4 heart failure patients (25%) are typically readmitted to hospital within 30 days of their discharge, and most of them are readmitted within 6 months after initial hospitalization.⁴ These readmissions are often attributable to factors such as improper medical treatment, inadequate follow-up, and non-adherence to recommended diets.^{1, 3}

1. Monitoring Heart Failure

Current strategies for monitoring heart failure are not accurate and effective. They are mainly based on physiological parameters such as heart rate, weight, or blood pressure.^{5, 6} Checking your heart rate is a good way to gauge your health. It gives an overview of heart muscle function; however, variation in heart rate cannot be specifically linked to heart failure. Monitoring body weight daily can provide a warning sign that the body is not functioning well and holding on

to fluid. Nonetheless, this method lacks specificity and might not provide a guideline on lifestyle management. Finally, blood pressure can provide information about potential hypertension and, as a consequence, cardiovascular risk. It is a warning signal but may not always lead to heart failure. To be proactive and accurately monitored, patients must go to hospital, spend time standing in line, and wait for blood test results. Overall, the process is long and uncomfortable for patients and patients may not be able to get help on time.

Monitoring heart failure markers at home could significantly improve patients' quality of life and their daily routines. Thus, it would be important to develop a tool to help patients and their physicians monitor health status from home. Monitoring HF at home is challenging because of the necessity to detect various biomarkers in a complex medium and not rely only on physiological parameters.⁷ According to recent clinical studies, creatinine is one of the promising biomarkers because of its primary role in heart failure and kidney disease.^{8,9}

A good practical example of how such technology may function is the widely used glucose meter. It provides rapid, accurate, and affordable blood sugar testing for patients who are suffering from diabetes.^{10,11} The glucometer, a groundbreaking technology developed more than 40 years ago, allows patients to self-monitor glucose fluctuations multiple times per day in order to successfully manage their personal treatment.¹⁰ People living with diabetes use glucometers to determine how much insulin to take, evaluate the body's response after physical exercise, and adjust their lifestyle accordingly. Daily blood sugar is measured in a single drop of blood as part of patient's routine. Thus, similar technology would be ideal for monitoring creatinine on a regular basis at home.

1.1. Creatinine: an important biomarker to assess renal function and predict heart problems

Creatinine is a small molecule generated as a waste product from muscle metabolism.¹¹ It is a clinically relevant biomarker because the creatinine molecule is not metabolized or reabsorbed by the kidneys. Therefore, a creatinine test assesses kidney function in clinical laboratories and can help predict heart failure.

Creatinine is a by-product of creatine breakdown and is formed by a multistage synthesis. The process takes place mainly in the liver, the kidneys and the pancreas.¹² The biosynthesis of creatine and creatinine is presented in Fig. 1. Creatine is synthesized through two enzymes glycine amidinotransferase (AGAT) and guanidinoacetate methyltransferase (GAMT) that mediate reactions involving three amino acids: L-arginine (Arg), glycine (Gly) and S-Adenosyl methionine (SAM). The transfer of an amidino group from Arg to Gly forms ornithine and Guanidinoacetate (GAA); it is the first stage of the biosynthesis of creatine. In the second stage, GAA is methylated at the amidino group and leads to creatine (Fig. 1A).¹³ Creatinine can be non-enzymatically hydrolyzed and cyclized into creatinine irreversibly. This reaction is temperature and pH-dependent.¹⁴ On the other hand, creatine can be reversibly phosphorylated by an enzyme (creatinine kinase, CK) to make phosphocreatine (Fig. 1B). This process is highly energetic and requires adenosine triphosphate (ATP). Later, phosphocreatine can be spontaneously broken down to creatinine during a nonenzymatic cyclization reaction.

The presence of creatinine in the blood signals kidney dysfunction, which can lead to heart failure. Heart failure has a direct impact on renal function because healthy kidneys depend on vascular health. High blood pressure can cause changes in small blood vessels, such as dilation or constriction. Thus, the kidneys cannot remove waste products from the blood, and high creatinine levels become a signal of the inability to maintain the cardiovascular system.

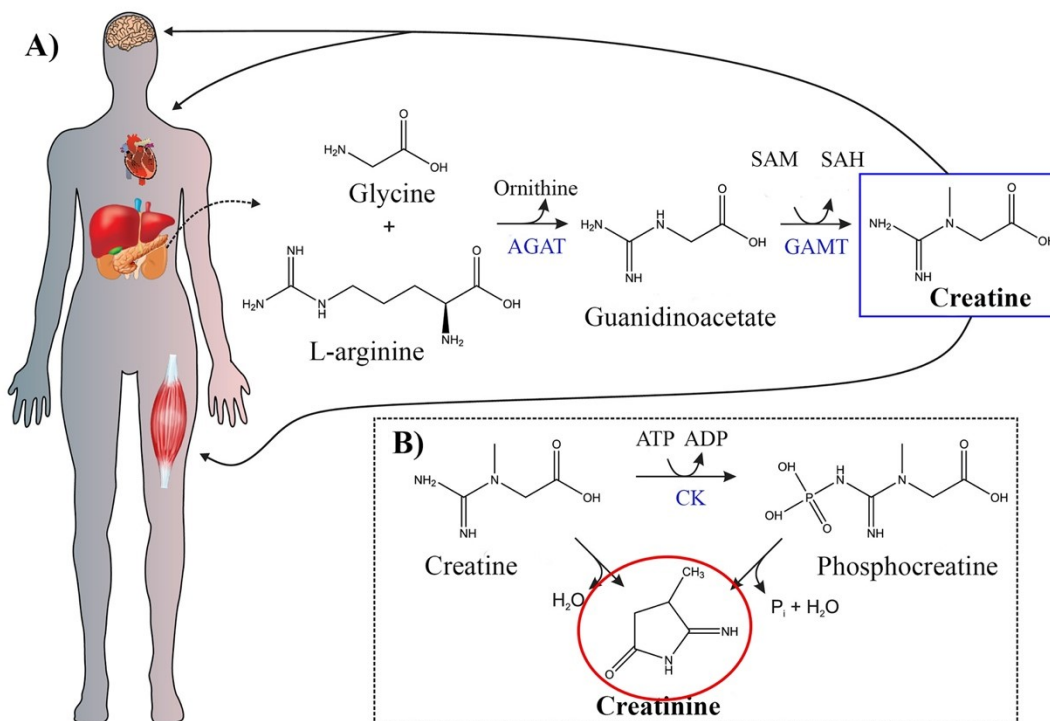


Figure 1. Biosynthesis of creatine. A) Scheme of creatine biosynthesis, and B) Creatine is metabolized to creatinine (CRT) through two possible reactions. The figure was taken without modification.¹³

How can physicians make a conclusion about bodily dysfunction and diagnose kidney disease linked to heart failure? First of all, there are two principal ways of measuring creatinine levels: in blood or in urine.¹⁵ In blood, it is called “serum creatinine”, and physicians measure its concentration to test kidney function. On the other hand, a urine test indicates the amount of creatinine which has passed through the kidneys into the urine. Two main parameters obtained from creatinine measurements can be considered as reliable indicators of renal function and a good predictor of heart problems.⁹ The efficiency of creatinine filtration is called the creatinine clearance rate, and with this rate, it is possible to estimate glomerular filtration rate (GFR). GFR is the rate of blood flow that is filtered by the glomerulus and shows how well the kidneys are functioning.^{15, 16} If a physician knows the exact concentration of creatinine either in blood or in urine, GFR can easily be calculated to diagnose the functioning of the glomeruli and the stage of kidney malfunction. Usually, the creatinine concentration in urine ranges from 20 to 275 mg/dL

(the equivalent of 1.7 – 24.3 mM).¹⁷ Patients typically store their urine in a special jug for one day and return it to the hospital or clinic for analysis. This test is inconvenient and requires careful sample collection. In contrast, a blood test involving the prick of the finger seems relatively rapid and easy to perform. The optimal range of creatinine in serum is 0.6-1.2 mg/dL (equivalent to 53-106 μ M).¹¹ A concentration higher than 106 μ M is associated with the risk of heart disease. The patient should consult a physician or go to a hospital for treatment. A concentration lower than 53 μ M can indicate abnormal renal function. Therefore, having a sensor at home could prove useful.

Monitoring heart disease typically requires a holistic approach to achieve better clinical outcomes. Ideally, several markers should be considered at the same time (e.g., creatinine, B-type natriuretic peptide (BNP), N-terminal fragment of its prohormone (NT-proBNP), hemoglobin, troponin I, etc.).^{7, 8, 18} Taken together, these biomarkers allow one to assess risk and provide accurate feedback to clinicians and patients.

1.2. Current state-of-the-art detection of creatinine

There are several techniques currently used to estimate creatinine concentration in clinical laboratories. These techniques are based on enzymatic or non-enzymatic reactions.¹⁹

1.2.1. Chemical method based on Jaffe's reaction for detection of creatinine

One non-enzymatic method is the Jaffe reaction. It is a colorimetric assay using ultraviolet-visible (UV-Vis) spectrophotometry. In this reaction, creatinine and picric acid form the orange-red Janovsky complex in an alkaline environment that can be detected and quantified at a wavelength of 510 nm (Fig. 2). This method is widespread due to its simplicity and low cost for determining GFR. In fact, it has been used for more than 136 years.²⁰

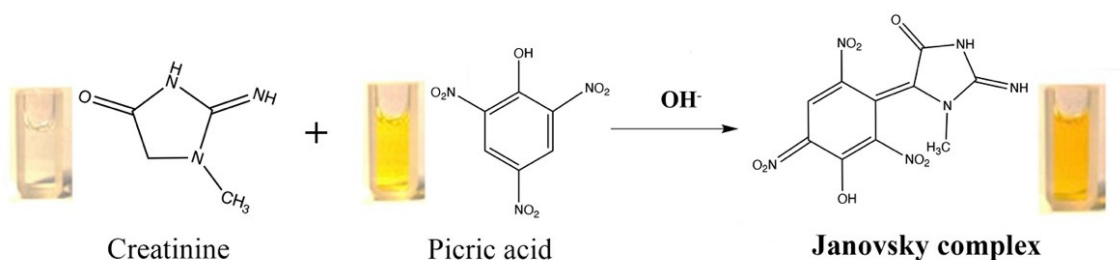


Figure 2. Jaffe's reaction. Creatinine (colorless) forms an orange-red complex with picric acid (yellow), called the Janovsky complex. The figure was taken without modification.²¹

However, this detection method has some disadvantages. One of the main drawbacks is that it is not specific to creatinine. Other metabolites in the patient's sample (serum and/or urine) have been shown to form coloured complexes with alkaline picric acid (e.g. bilirubin, glucose, hemoglobin, and some proteins).^{16, 19} Consequently, these non-creatinine-related chromogens lead to a 15-25% higher signal than creatinine.^{22, 23} Moreover, it is a time-consuming method that requires sample pre-treatment involving centrifuging and pipetting solutions. Also, the method needs more than 0.15 mL of a biological sample.

1.2.2. Enzymatic strategies for the detection of creatinine

As no alternative chemical methods were found, enzyme-based assays were developed. The main advantage of using enzymes to detect creatinine is their high selectivity, as they do not react with other molecules in biological samples. However, finding the right enzyme may be challenging. Particularly, to detect the creatinine molecule, clinical laboratories often use the combination of two or three enzymes to improve the assay's specificity increasing the cost of the routine analysis.¹⁹ Typically, enzymatic strategies for detecting creatinine are based on three well-known reactions (Fig. 3).²² In the enzyme-based creatinine sensors, an enzyme cleaves a substrate (creatinine), and the product of the reaction generates a measurable signal. The measurable signal can be obtained through detecting a by-product of the reaction, such as H₂O₂, cation ammonium (NH₄⁺) or ammonia (NH₃), using a specific transducer. Therefore, the concentration of creatinine depends on the initial substrate concentration as well as on the enzyme activity.

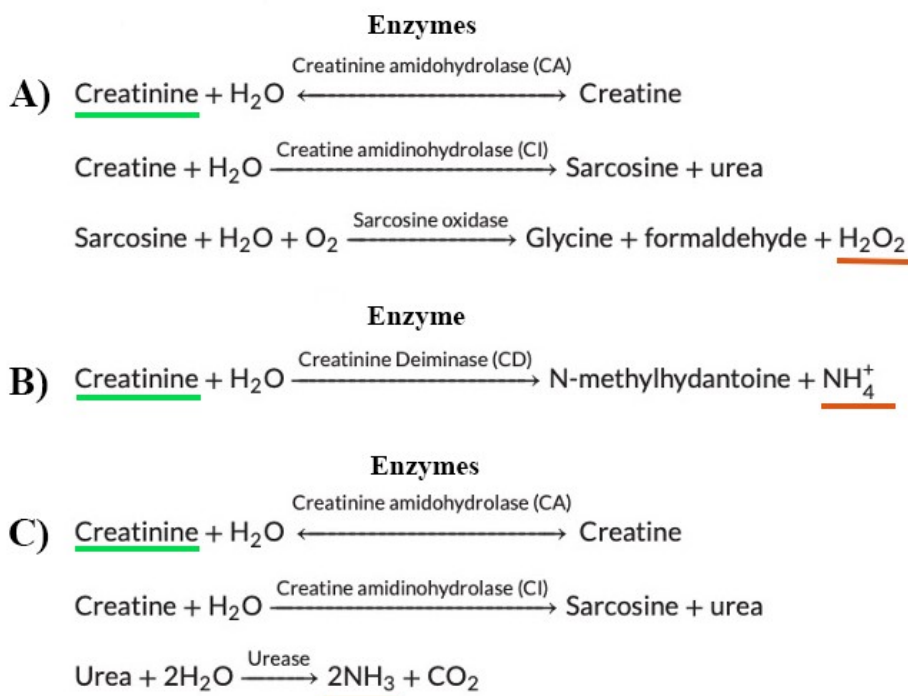






Figure 3. Examples of three main enzymatic reactions to detect creatinine. The figure was taken without modification.²²

Today, an effort is made to implement the use of quick and relatively portable electrochemical sensors with enzymes in current devices; however, there is still room for improvement, and they are yet to be optimized. As we may see from Table. 2, these devices are not user-friendly because they remain typically too expensive to be employed at home (>4000\$) and often require special assistance.²³⁻²⁶ Reflecting on these facts, biosensors could be a good alternative to facilitate patients' daily routines by enabling them to monitor their markers in the comfort of their home.¹³

Table 2. Comparison of the point-of-care devices based on enzymatic reactions coupled with the electrochemical reader.

Characteristics	StatSensor ²³	i-STAT ²⁴	ABAXIS PICCOLO Xpress ²⁵	Epoc Blood Analysis ²⁶
Design				
Volume	1.2 µL	65 µL	100 µL	92 µL
Time	30 sec	2 min	< 14 min	1 min
Price	4000 CAD + strips 700 CAD (14 CAD per test) ²⁷	4500 CAD + cartridge 200 CAD (19 CAD per test) ²⁸	5200 CAD ²⁹ + reagent disk 200 CAD (20 CAD per test) ³⁰	7000 CAD + card 1400 CAD (28 CAD per test) ³¹

1.3. Biosensors as promising diagnostic devices

1.3.1. What is a biosensor?

A biosensor is an analytical device that uses a biorecognition element (bioreceptor) to bind a target molecule (referred to as the binding event) and a chemical or physical transducer to process and produce a measurable signal (signal output) (Fig. 4).^{32, 33} Various biorecognition elements have been employed in different biosensors, including enzymes, antibodies, nucleic acids or cells.³⁴ Upon specific recognition of the analyte, the binding event leads to the generation of an electrochemical, optical, thermal, spectroscopic, or another type of signal that can be transduced into a measurable readout.

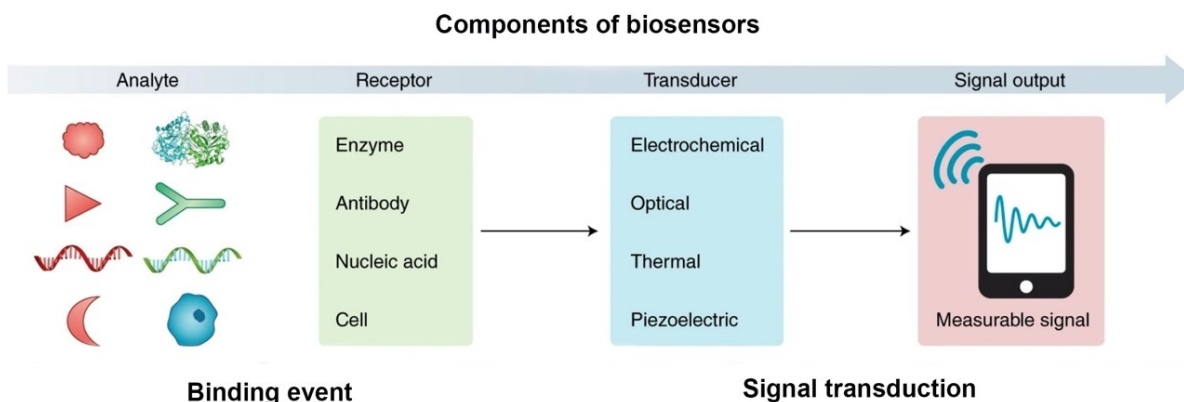
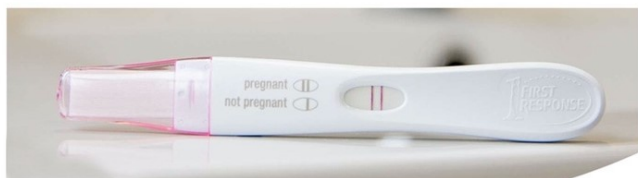


Figure 4. The scheme represents the main components of the biosensor. The figure was taken without modification.³⁵

Oftentimes, the purpose of developing a biosensor is to have a small device that can monitor an analyte of interest outside of a central laboratory. The analyte is typically a molecule or group of molecules present in saliva, blood, sweat or other biological fluids that can be detected with or without pre-treatment of the sample. Various biorecognition elements have been employed to build biosensors, including enzymes, antibodies, protein receptors, nucleic acids, or cells.^{33,36} These elements enable specific recognition of the analyte and can be coupled to various signalling mechanisms to transduce biomolecular binding into specific readouts (e.g., electric, colorimetric, etc.).^{33,37}

Biosensors represent a revolutionary solution in the medical field for improving patient health. According to recent research, the worldwide market size for point-of-care biosensors will reach \$43 billion by 2029.³⁸ This can be explained by the steadily growing number of lifestyle ailments (e.g., cancer, genetic disease, heart failure). Biosensors have already been successfully developed in clinical applications and compare favourably with other analytical devices.³⁹ To date, they range from the simple lateral flow immunoassay that uses antibodies for a recognition element (pregnancy test - Fig. 5A) to the portable glucometer that uses enzymes for a recognition element (glucometer - Fig. 5B).⁴⁰⁻⁴³ These biosensors are cost-effective and have been commercially available for more than 30 years.

A)



B)



Figure 5. Commercially available biosensors. A) Pregnancy test (Lateral flow immunoassay), B) Glucometer (electrochemical enzyme-based sensor). These figures were taken without modification.^{44, 45}

Although enzyme-based sensors (e.g., glucometers) have seen widespread use for treating diabetes, their working mechanism displays certain limitations. Firstly, enzyme-based sensors are not universal since they cannot be adapted to detect molecules that are not involved in a known enzymatic reaction. Secondly, enzymes are very sensitive to environmental conditions and may not work well in complex matrixes (e.g., blood, urine, sweat, etc.). Lastly, enzymatic activity

depends on the quality and immobilization of enzymes, which requires laborious development to achieve reproducible fabrication and suitable shelf-life.⁴⁶⁻⁴⁸

Despite their great success, antibody-based sensors (e.g., pregnancy tests) also display many limitations. Similar to enzyme-based assays, antibody-based sensors can also be sensitive to environmental conditions. The main limitation of antibody-based sensors, such as lateral flow immunoassays, is that signalling mechanisms employed in this class of sensors generally provide qualitative or semi-quantitative results. The device only provides a “yes or no” answer. Thus, it is not applicable to determine the precise concentration of molecules which is needed for various health applications, such as glucose or creatinine monitoring.

In order to develop sensors that would provide the most benefits for future applications, the World Health Organization has concluded that the ideal biosensor should possess the following characteristics:^{49, 50}

- 1) Sensitive and specific,
- 2) Quantitative,
- 3) Work in a complex medium (e.g., whole blood, saliva, urine),
- 4) User-friendly (ease-to-use),
- 5) Cost-effective (manufacturable),
- 6) Rapid,
- 7) Versatile.

1.3.2. Electrochemical DNA-based sensors

1.3.2.1. Background

Electrochemical biosensors are a subclass of chemical sensors that transduce the molecular binding event into the generation of an electrochemical signal.⁵¹ The main advantages of electrochemistry are exemplified by the glucometer. The glucometer is cheap, rapid, quantitative, portable, and provides a signal in complex samples such as serum or whole blood. We note that electrochemical detection has achieved widespread use in clinical analyses due to the abovementioned characteristics. Thus, biosensors coupled with electrochemical methods are becoming an efficient and promising tool for analytical application.

1.3.2.2. E-DNA sensor

Electrochemical DNA-based (E-DNA) sensors represent a group of biosensors that utilize DNA either as a biorecognition element or as a signalling mechanism to convert a biological reaction into a measurable electrochemical signal.^{52, 53} The first electrochemical DNA (E-DNA) sensor based on target binding-induced folding of attached DNA probes was introduced by Plaxco and Heeger in 2003. The 5' terminus of a short single-stranded DNA that formed a stable stem-loop architecture was covalently attached to a redox reporter, and its 3' terminus was covalently attached to a thiol moiety for immobilization onto a gold surface via a gold-thiolate bond. A complementary DNA strand binds to the E-DNA sensor triggering the opening of the hairpin and the removal of the redox reporter, methylene blue, far from the gold surface (Fig. 6).⁵⁴ This results in a decrease in the Faradaic current due to reduced electron transfer efficiency. This biosensing architecture was reported to detect less than 10 pM of the target, demonstrating that electrochemical DNA-based sensing can provide highly sensitive detection.

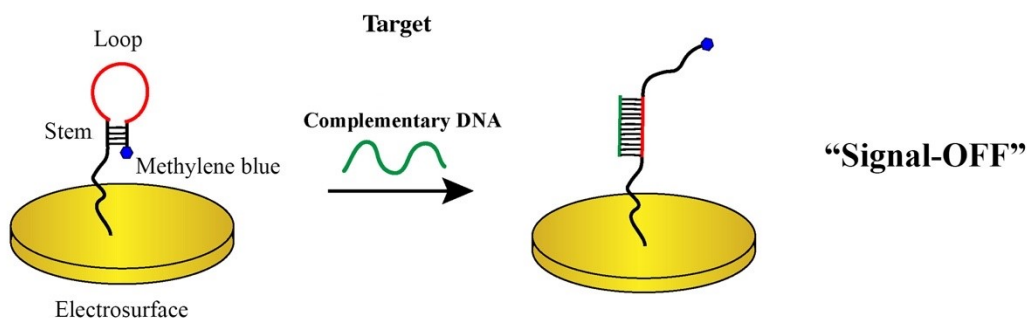


Figure 6. One component E-DNA sensor based on DNA hybridization. The detected target is a DNA fragment of complementary sequence. The figure was adapted from Plaxco *et al.*⁵⁴

The main limitation of such a sensing architecture, however, is that the signalling mechanism displays a “signal-OFF” electrochemical output, meaning that the sensor signal decreases with increasing analyte concentration. “Signal-ON” sensor architectures are generally considered more reliable because the generated signal does not interfere with various artifacts that decrease the signal (e.g., non-specific binding, sensor degradation).⁵⁵ It is therefore preferable to have a “signal-ON” sensor because the signal is generated by detecting a specific molecule, and there is no loss of the initial current. Another limitation of the above-mentioned sensing architecture based on DNA hybridization is that it cannot be applied to detect non-nucleic acid targets such as proteins.

1.3.2.3. Electrochemical Aptamer-based sensors (AB-sensors)

In order to further expand the universality of E-DNA sensors in terms of the variety of target analytes, Plaxco *et al.*⁵⁴ also introduced electrochemical aptamer-based (E-AB) sensors. Aptamers are single-stranded DNA or RNA sequences consisting of around 20-80 nucleotides (nt) that have been selected to fold and bind to a specific target analyte. An aptamer’s binding ability does not depend on the chemical reactivity of the target; therefore, the most important advantage of using DNA as a biorecognition element sensor is that it can cover a range of targets, including ions, small molecules, proteins, and even cells.^{36, 56-58} These aptamers are generally designed or identified using a selection strategy first introduced in 1990 called Systematic

Evolution of Ligands by Exponential Enrichment (SELEX) (see section 1.3.3 for more details on SELEX).^{59, 60} Since then, the SELEX method has been dramatically improved, with the possibility of selecting aptamers against various target molecules with high affinity and specificity.^{61, 62} In 2005, the group of Kevin Plaxco adapted one of these aptamers into an E-AB sensor for the sensitive, selective, and rapid detection of thrombin.⁶³ Using this sensor, they demonstrated the detection of 64 nM of thrombin directly in bovine serum. Their sensor design is relatively simple (Fig. 7A). A short single-stranded aptamer containing a redox element is first immobilized on a gold electrode using a gold-thiolate bond. In the absence of the target, the aptamer remains unfolded, and the redox element (methylene blue) is able to reach the gold electrode and transfer its electrons efficiently. Upon binding to the thrombin protein, the aptamer folds into a G-quadruplex conformation (formed from four stacked guanine), significantly altering electron shuttling, thus creating a “signal-OFF” sensor.

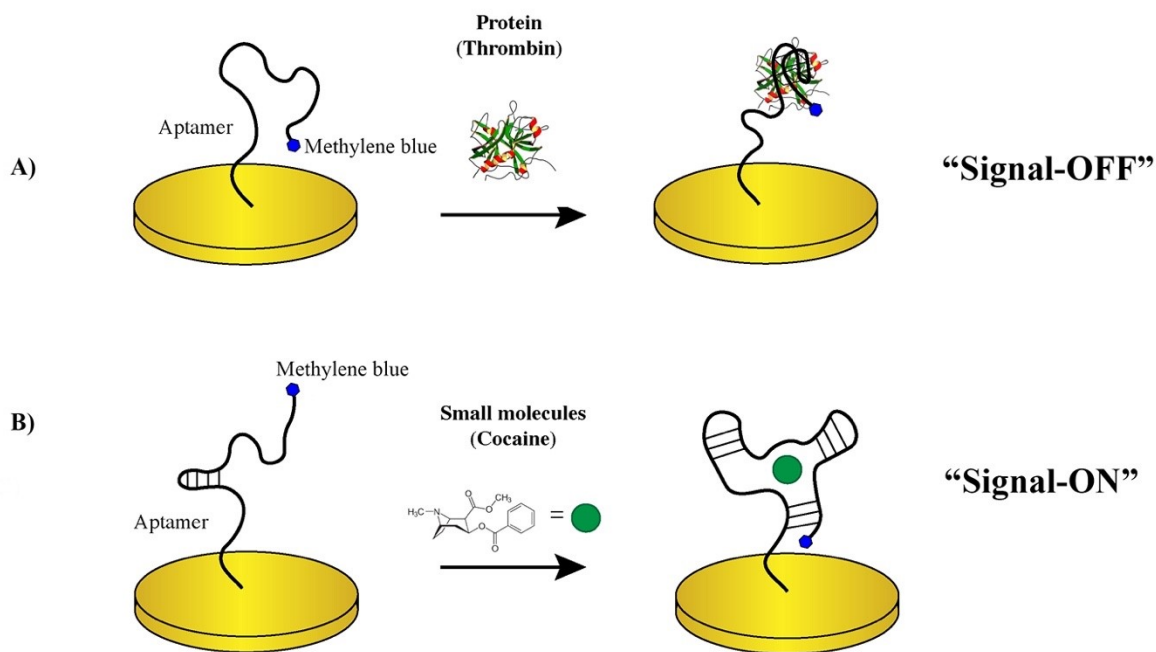


Figure 7. E-AB sensors based on binding-induced conformational changes. Detected targets are: A) thrombin and B) cocaine. Detection of thrombin and cocaine are based on their specific aptamers. These sensors are generally referred to as one-component sensors since they

combine both the recognition mechanism and the signalling mechanism in a single component. The figure was adapted from Plaxco *et al.*^{63, 64}

One year later, the same group also adapted this strategy to the detection of small molecules (e.g., cocaine) by creating a “signal-ON” sensor.⁶⁴ They fabricated this sensor using a structure-switching mechanism similar to the one mentioned above (Fig. 7B). In the absence of the target, the aptamer remains partly folded, and the redox element transfers electrons with reduced efficiency. Upon binding to cocaine, the aptamer folds and brings a redox element closer to the gold surface, thus producing a “signal-ON” output. It is worth noting, however, that the performance of these E-AB sensors is also strongly dependent on the length, the secondary structure, and the stability of the aptamers employed. Indeed, in order to be efficient, these biosensing architectures require careful optimization of the folding energy of the aptamers.⁶⁵ More specifically, the aptamers must remain relatively unfolded in the absence of the target without being too destabilized.

1.3.2.4. Kinetically programmed aptamer-based sensors

Another promising strategy, the “kinetically programmed DNA assay”, was developed by Guichi Zhu from our laboratory of Biosensors and Nanomachines.⁶⁶ He has been developing a universal aptamer-based strategy for detecting any specific targets in a single-step assay. His strategy employs a kinetically programmed hybridization assay where an aptamer, a signalling DNA strand, and a capturing DNA strand are added together simultaneously (Fig. 8). This approach relies on their different binding kinetics. Thus, three competitive reactions occur which can form the complexes target-aptamer (T-A), aptamer-signalling DNA (A-S), and signalling DNA-capturing DNA (S-C). So, in the presence of a target, the target rapidly sequesters the aptamer (also called the recognition reaction, k_1), and the signalling strand cannot hybridize with the aptamer (this reaction is called the inhibition reaction, k_2). As a result, the signalling DNA has no other choice but to bind to the complementary capturing DNA located on the surface of the electrode (also called the signalling reaction, k_3). This results in the generation of an electrochemical signal. In contrast, in the absence of the target, the aptamer will hybridize with the signalling DNA strand, so only a few available signalling DNA strands will be able to reach the surface and hybridize with

the capturing DNA strand. This biosensor is able to get a high, observable signal gain of 100 % after 5 min of reaction. Having $k_1 > k_2 > k_3$ leads to successful performance since the aptamer binds more rapidly to the ligand compared to the signalling DNA strand. More importantly, this mechanism is not affected by non-specific interactions and provides relatively fast hybridization.

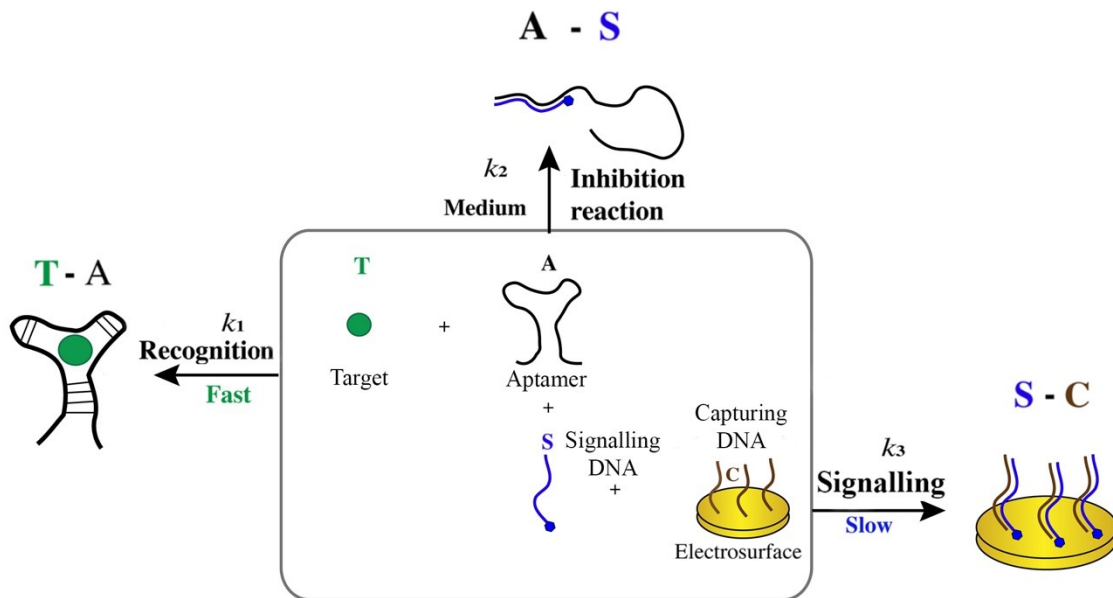


Figure 8. Representation of the new kinetically programmed strategy. Three components (target, aptamer, and signalling DNA) are added simultaneously to the capturing DNA attached to a gold surface. The figure was adapted from Zhu *et al.*⁶⁶

The number of publications in the field of biosensors continues to rise steadily, and researchers keep exploring ways to translate novel sensing architecture into point-of-care devices. Despite noteworthy advances in electrochemical aptamer-based sensors, the reported architectures remain limited by various challenges. For example, as we have seen before, Plaxco’s strategy (Chapter 1, section 1.3.2.3) requires an individual optimization of the aptamer’s folding energy. It is therefore hard to control when creating a “signal-ON” or “signal-OFF” sensor.^{63, 64} Of note, thermodynamics play a pivotal role in this particular biosensing architecture. Additionally, an important consideration is the surface density of immobilized aptamers. It should be optimized

individually to avoid steric hindrance. Moreover, sensor aging drastically affects the intensity of the signal. The strategy proposed by G. Zhu likely solves these limitations and systematically increases the gain of the assay. However, as we will see later, even this kinetically programmed strategy is not found to be as universal.

1.3.3. Novel aptamer-based signalling mechanism based on selection strategies

New sensing strategies are often described as being “universal”. In fact, many strategies are not universal at all, and they still face challenges. More specifically, none of the aforementioned strategies have been universal for detecting a large variety of targets. As we can easily observe, none are used as universal sensors on the commercial market. Our motivation behind developing universal electrochemical aptamer-based biosensors is to make the assay more adaptable to the detection of any target with minor optimization. Therefore, we started with an in-depth analysis of how aptamers are selected. We were inspired by the idea of whether we could imitate the selection process to design a new sensing architecture.

1.3.3.1. Conventional aptamer selection strategies

In general, selection strategies select for optimal activity. In the case of aptamers, they are selected based on their binding affinity to a specific target molecule (ions, toxins, drugs, peptides, proteins, cells, etc.). What is often forgotten, however, is that typically selection strategies also select for a specific structure-switching mechanism.⁶⁷

SELEX typically starts with a random library of single-stranded nucleic acids (DNA or RNA) attached *in vitro* by solid-phase synthesis (Fig. 9). The screening library is based on random sequences from 20 to 80 nt flanked by two conserved regions at the 5' and 3' extremities (15-25 nt). The process begins with incubating a “random library” (usually 10^{15} sequences) and a target under desired conditions. After washing out unbound sequences (elution step), bound sequences move on to the partitioning round. This step helps to remove loosely bound aptamers (with low affinity to the target) and find sequences displaying strong interactions. The partitioning round is the most challenging and, at the same time, is a very diverse step. It can be done either by attaching an aptamer to a solid support (e.g., beads, sepharose) or binding in solution. Usually, counter and negative selections occur during this selection period to identify an aptamer with

better selectivity.⁶⁸ Counter-selection is performed against molecules with similar structures and chemical groups to improve aptamer selectivity and affinity. Negative selection is performed to avoid interference of non-target bound aptamers and enhance working efficacy under desired reaction conditions.⁶⁹ Negative selection is helpful when we need to work in a special environment in the sample (e.g., acidic pH, specific ions, complex biological samples, etc.). When it comes to working in a complex matrix such as serum, whole blood or saliva, we want to ensure that the aptamer will specifically and selectively bind to the target of interest and not bind to other molecules. The specific aptamer sequences are then amplified via polymerase chain reactions (PCR). Single-stranded DNAs are regenerated from PCR to constitute a new pool called the enriched library. This pool undergoes all steps again until the resulting aptamer pool is sufficiently enriched. During the last SELEX round, the enriched pool is cloned and sequenced.⁵⁸

70

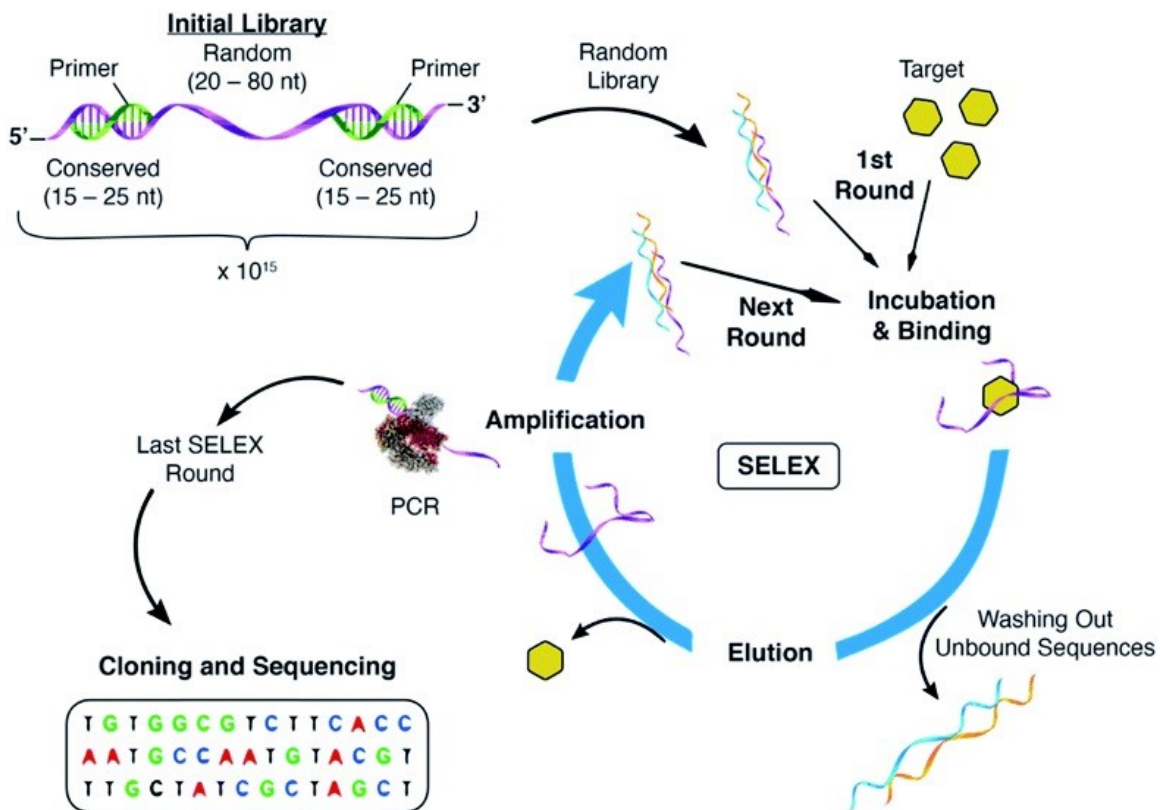


Figure 9. General scheme of SELEX (Systematic Evolution of Ligands by Exponential enrichment) process with main steps. See the main text for more details. The figure was taken without modification.⁵⁸

1.3.3.2. A capture-SELEX strategy

A capture-SELEX is a variant of conventional SELEX. Recently, this type of SELEX has been getting much attraction because it allows for designing aptamers against different molecules, particularly small molecules (Fig. 10).⁷¹⁻⁷³ In this selection approach developed by the Stojanovic lab, the “designed DNA library” consists of two strands: a capturing strand and an aptamer. Each strand of the “aptamer library” contains a capturing strand-binding region, a random region, and a competitive stem region that directly participates in the structure-switching of the aptamer in the presence of the target. Here, a capturing strand from the selection (*blue line*) is attached via biotinylated DNA to an agarose-streptavidin column. This capturing strand is complementary to the capturing strand binding region of the random sequence of the “aptamer library” (*green line*). If no binding happens, then there is no induced conformational change, and the aptamer still attaches to its complementary capture strand.⁷⁰ However, upon binding to a target, the target induces dissociation of the aptamer from the capturing strand. The aptamer changes its conformation and releases the short capturing strand from the selection. This is called a partitioning mechanism. The unbound sequences are removed by washing several times. Conversely, the bound sequences are amplified by PCR for large-scale cloning and sequencing as in conventional SELEX.

The main advantage of the capture-SELEX is that it is well-suited to selecting aptamers for small molecules (e.g., creatinine).^{74, 75} Often small molecules cannot be immobilized on a solid surface. However, in this method, the library of DNA sequences is attached to the support instead of the targets; therefore, there is no need to modify the target chemically. Another advantage of this method is that using unmodified small targets can increase possible interactions with the aptamer and therefore improve its binding affinity. And lastly, using the capture-SELEX method allows for adapting the structure-switching mechanism in a fluorescent screening assay that is based on the selection.^{61, 68, 75}

Recently, this capture-SELEX has become popular due to its ease of being adapted into a fluorescence-based sensor.^{71, 76-78} A few detailed examples are presented in Fig. 11. For example, Y. Li designed a novel approach to transform the capture-SELEX into a fluorescence signalling system. In his strategy, the sensor consists of three DNA strands: an unlabelled aptamer, a strand with a fluorophore (F), and one strand with a quencher 'capture strand' (Q). The latter strand is a good example of imitating a complementary 'capturing strand' from the selection. The Li group designed strands based on DNA's complementarity; therefore, two parts of the aptamer are complementary to the strand with the fluorophore and the quencher (Fig. 11A). Specifically, the three mentioned strands stay intact, remain quenched, and do not produce a signal (low fluorescence). However, in the presence of a target molecule, the aptamer changes its conformation, detaches the capturing strand, and increases a fluorescence signal (high fluorescence).⁷⁹

Another successful example of the adaptation of the capture-SELEX strategy into molecular beacon aptamers was demonstrated by the Group of Morse in 2007 (Fig. 11B). Morse chemically labelled the aptamer with a fluorophore at its 5' extremity, and the capturing strand (the same strand that comes from the selection) was labelled at its 3' extremity. When no target is present, the two complementary strands form a duplex and stay together, leading to a low fluorescence signal. However, upon binding to the target, the introduced target induces a conformational change of the aptamer leading to a high fluorescent signal.⁸⁰ This specific labelling (like a molecular beacon) was well explored and incorporated in an efficient aptamer's screening by many other groups.^{72, 81, 82}

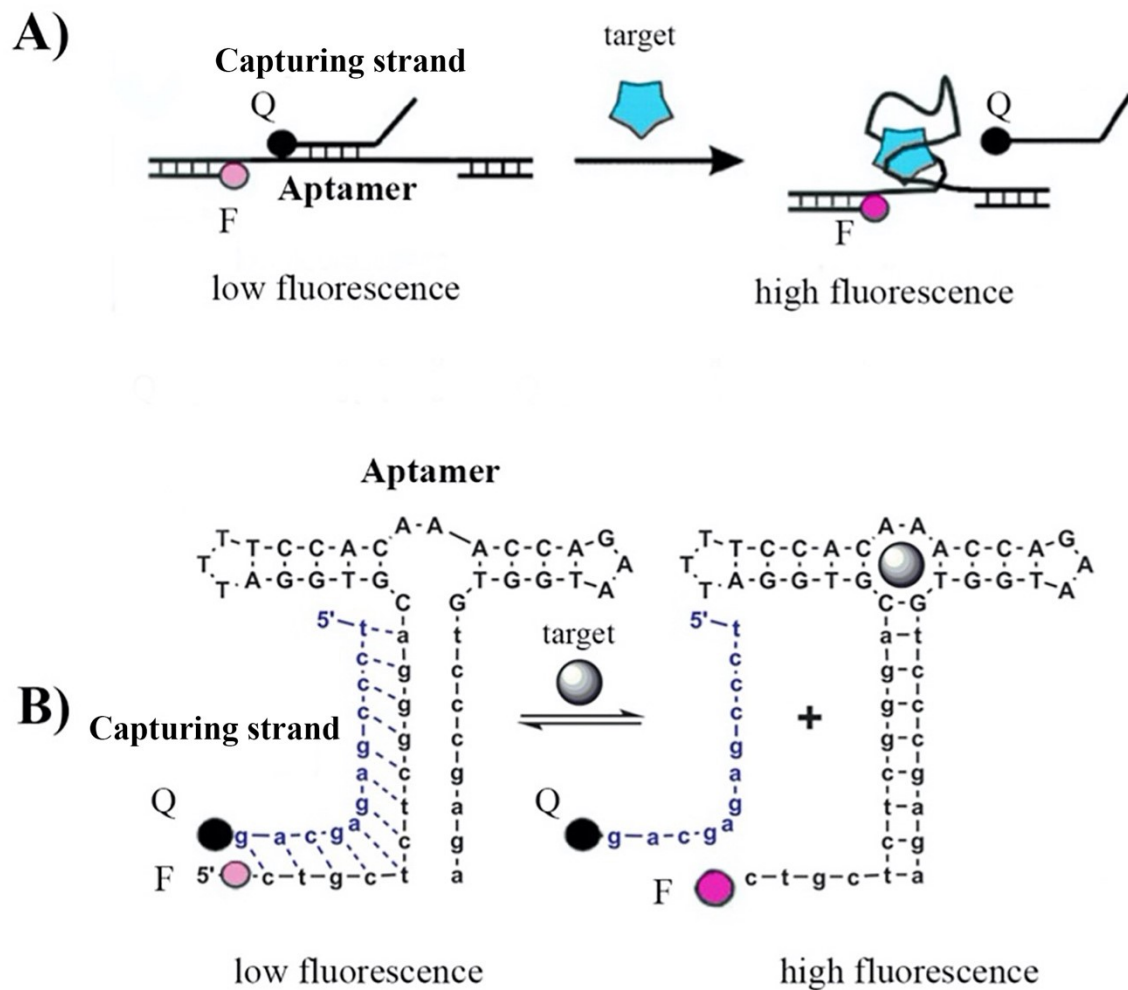


Figure 11. Capture-SELEX strategies enable easy adaptation into a fluorescent sensor. A) Y.Li *et al.*⁷⁹ designed a variation involving an immobilized capturing strand that hybridizes within the aptamer's random region and dehybridizes in the presence of a target molecule. B) Morse *et al.*⁸⁰ demonstrated the adaptation of capture-SELEX into molecular beacon aptamers. The introduced target induces a conformational change of the aptamer and leads to the dissociation of the two strands (aptamer and a short capturing strand). These figures were taken without modification.^{79,80}

1.4. Aim and thesis structure

The capture-SELEX strategy is an alternative aptamer selection method for binding targets with high affinity without disrupting the natural state of the targets. We decided to take advantage of this strategy and hypothesize that the already optimized structure-switching mechanism selected from this approach could be readily adapted into an effective electrochemical sensing strategy (Fig. 12). Therefore, the aim of this project is to develop a sensing mechanism for creatinine based on the capture-SELEX selection strategy.

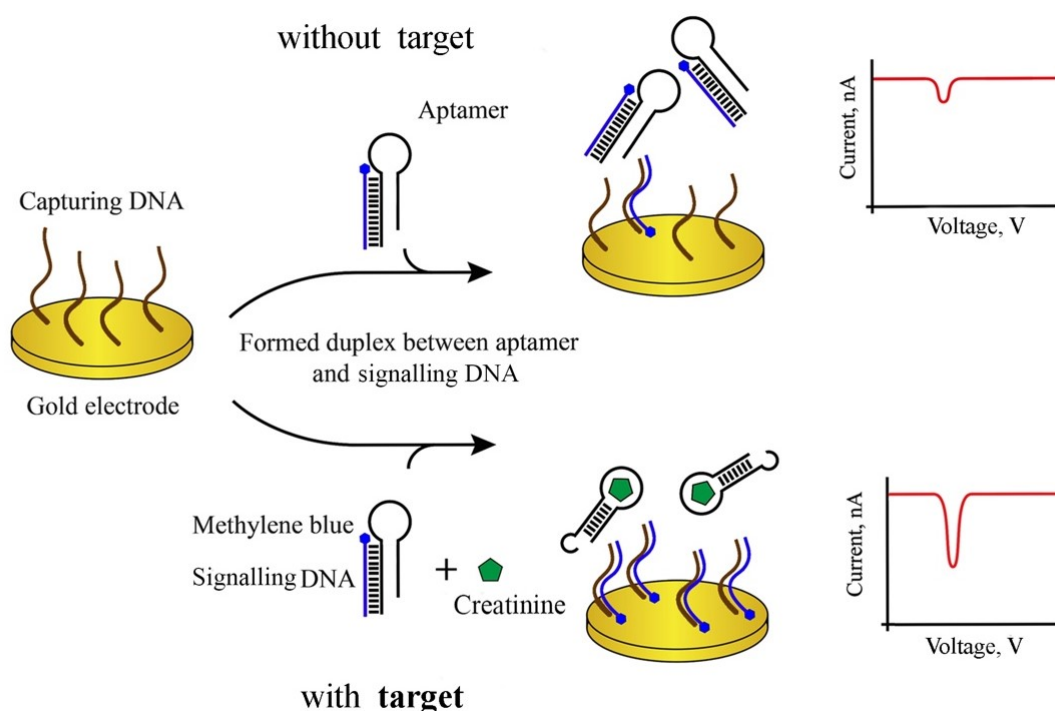


Figure 12. Designing an aptamer-based signalling mechanism based on its selection strategy (capture-SELEX). *Top:* In the absence of the target (creatinine), the signalling DNA, containing a methylene blue redox element, stays bound to the aptamer and cannot reach the gold electrode surface (low electrochemical signal). *Bottom:* In the presence of the target, the duplex formed between the signalling DNA and the aptamer dissociates, releasing the signalling DNA that can hybridize with the capturing DNA on the electroactive surface (high electrochemical signal).

To reach that aim, we must achieve specific objectives. Therefore, we first identified and characterized an aptamer selected using a capture-SELEX strategy. Then we adapted the aptamer into a sensing architecture, optimizing and tuning different parameters. And finally, we validated the sensor, spiking the molecule of interest (creatinine) in a complex matrix.

This thesis is organized into four chapters:

Chapter 1 provided a background and literature review on monitoring heart failure, biosensors, and the aptamer SELEX strategies.

Chapter 2 described the main methodology and instrumentation setup that has been used to develop and characterize a creatinine biosensor.

In Chapter 3, we further discussed and interpreted the obtained experimental results in greater depth and their impact on the designed electrochemical strategy.

To conclude the thesis, Chapter 4 summarized the main results and proposed perspectives for future work.

Chapter 2 – Methodologies for the development of new electrochemical aptamer-based sensors

This chapter described the main methodologies and a detailed plan for developing a new strategy aimed at facilitating the successful development of an electrochemical aptamer-based sensor (Fig. 13). The first step involved in the design of such a sensor was to identify a high affinity and selective aptamer recognition element and characterize it (step 1, section 2.1). In this study, we also employed *UNAFold*, a computational software, which helped to understand how the aptamer may fold and estimated the main parameters (e.g., base pair composition and melting temperature). To measure the binding affinity between the target and the aptamer, we used Isothermal Titration Calorimetry (ITC). Then we proposed to design a sensing mechanism based on the selection process of the aptamer (step 2, section 2.2) and carefully synthesized, purified and quantified all the designed DNA strands (step 3, section 2.3). With all the strands in hand, the next step was to validate the new biosensing architecture via a simpler fluorescence experiment (step 4, section 2.4). For some well-known biosensing architectures, it is possible to move on directly to electrochemical experiments. However, in this work, we demonstrated how fluorescence experiments could help validate the binding-induced structure-switching mechanism of the aptamer. Once this mechanism was validated, we could then adapt this strategy for electrochemical detection (step 5, section 2.5). In order to start these electrochemical experiments, we need to carefully choose the electrode system and the redox element, functionalize the electrodes with DNA and choose the electrochemical technique. With this in mind, we needed to characterize and optimize the electrochemical parameters. The performance of the biosensor was evaluated using four analytical parameters: sensitivity, specificity, repeatability, and dynamic range (step 6, section 2.6). Finally, the ability to detect the analyte of interest was further assessed in a clinically relevant complex matrix: serum (step 7, section 2.7).

Roadmap of methodology to create a new sensing strategy

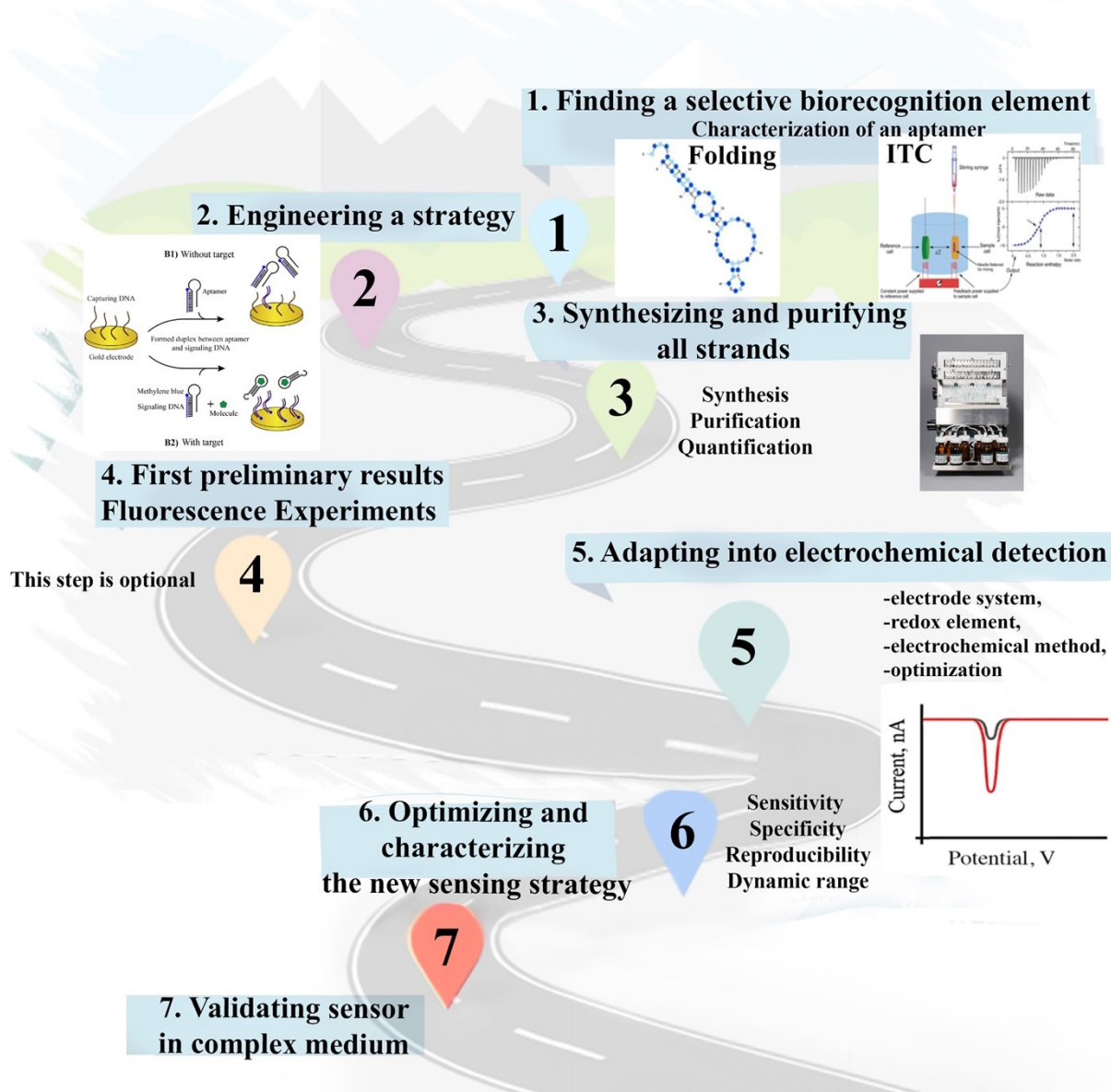


Figure 13. Overview of the methodology to create a new sensing strategy based on the capture-SELEX selection strategy. These essential steps are introduced and explained in Chapter 2.

2. Identifying a selective biorecognition element

We previously described creatinine as a good marker for HF problems. To recognize this small biomolecule, we identified a potential creatinine DNA binding aptamer developed by the group of Prof. Milan Stojanovic (Columbia University, USA). The SELEX strategy employed by Prof. Stojanovic relies on the capture-SELEX format already presented in Chapter 1, section 1.3.3.2. In order to explore the universality of our design strategy, we identified a moxifloxacin binding aptamer from the Aptamer Group Company (United Kingdom)⁸³ that has been also selected through the capture-SELEX strategy. Both aptamer's sequences are protected; therefore, their whole sequences are not shown in this thesis.

2.1. Analyzing DNA structure

Next, we aimed to better understand the secondary structure of the selected aptamers. To do so, we employed computational software such as *UNAFold* and *Integrated DNA Technologies Oligoanalyzer Tool*.^{84, 85} Folding predictions of the aptamers were performed at room temperature (23°C) under reaction conditions of 150 mM Na⁺, and 2 mM Mg²⁺. These analyses predicted a potential secondary structure of the aptamers (e.g., intramolecular stem-loop). Such knowledge was important to design and optimize the sensing architecture (step 2, section 2.2).

2.1.1. Measuring binding affinities using Isothermal titration calorimetry (ITC)

To estimate the binding affinity between the creatinine and its aptamer, we used an ITC instrument from GE Healthcare called MicroCal iTC 200 (Scientific platform BMM at Université de Montréal, department of biochemistry, faculty of medicine) (Fig. 14A). This physical technique is label-free, non-distractive, sensitive, and allows us to determine the quantitative thermodynamic parameters such as the variation in entropy (ΔS), the variation in enthalpy (ΔH), the free energy changes (ΔG), stoichiometry (n) and dissociation constant (K_d) through a computerized curve-fitting of the obtained data.⁸⁶ The K_d (dissociation constant) is a measure of the strength of the molecular interaction between creatinine and the aptamer and is defined by the concentration of creatinine at which 50 % of the aptamer is bound. Lower K_d values imply higher affinities

between the ligand and the biomolecule of interest, which means that even at a low concentration of creatinine, the binding event will happen.

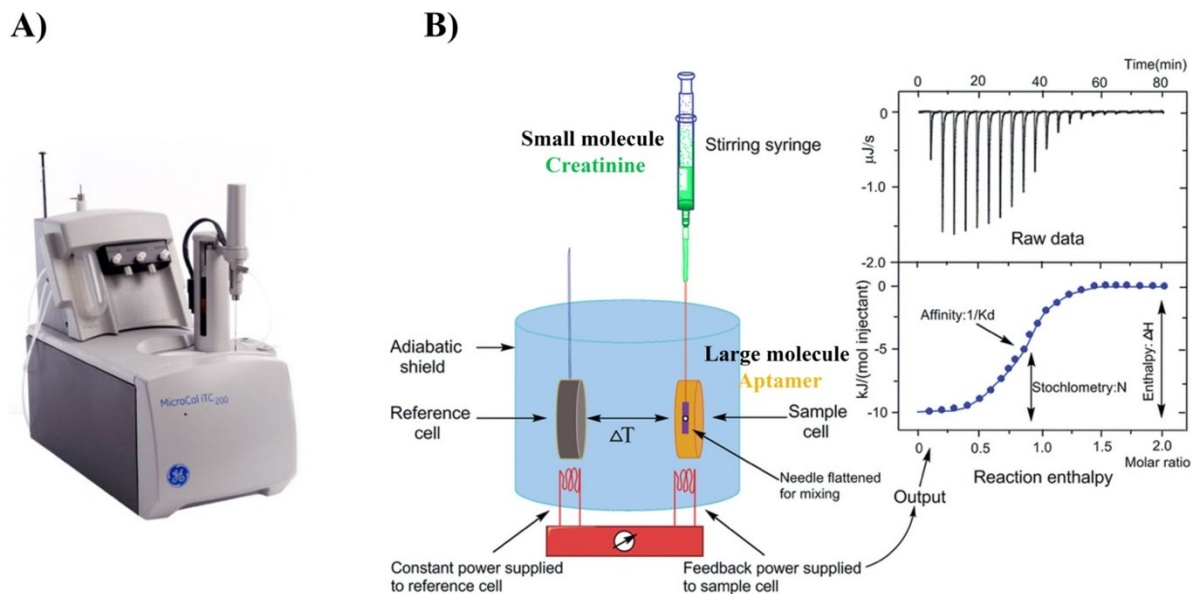


Figure 14. Overview of Isothermal Titration Calorimetry. A) GE Healthcare MicroCal iTC 200 B) ITC experimental design and data analysis (*Top*: raw data and *Bottom*: Wiseman plot). These figures were taken without modification.^{87, 88}

Briefly, the ITC instrument measures the heat variation (heat absorbed or released) involved in the molecular association (i.e., the binding of creatinine to its aptamer) that takes place in the cell during the titration. Usually, the larger molecule goes into the cell while the smaller one goes into the syringe (Fig. 14B). To determine the appropriate sample concentrations, we used an experimental design mode ‘Highest Quality’ and a c-value parameter from the standard software. The c-value is a concentration-dependent parameter that predicts the shape of the binding curve, its optimal value ranges from 10 to 500 (Fig. 15).⁸⁹ If the c-value is out of this range during computational design, it might lead to inaccurate results and, therefore, miscalculations of the association or dissociation equilibrium constants.

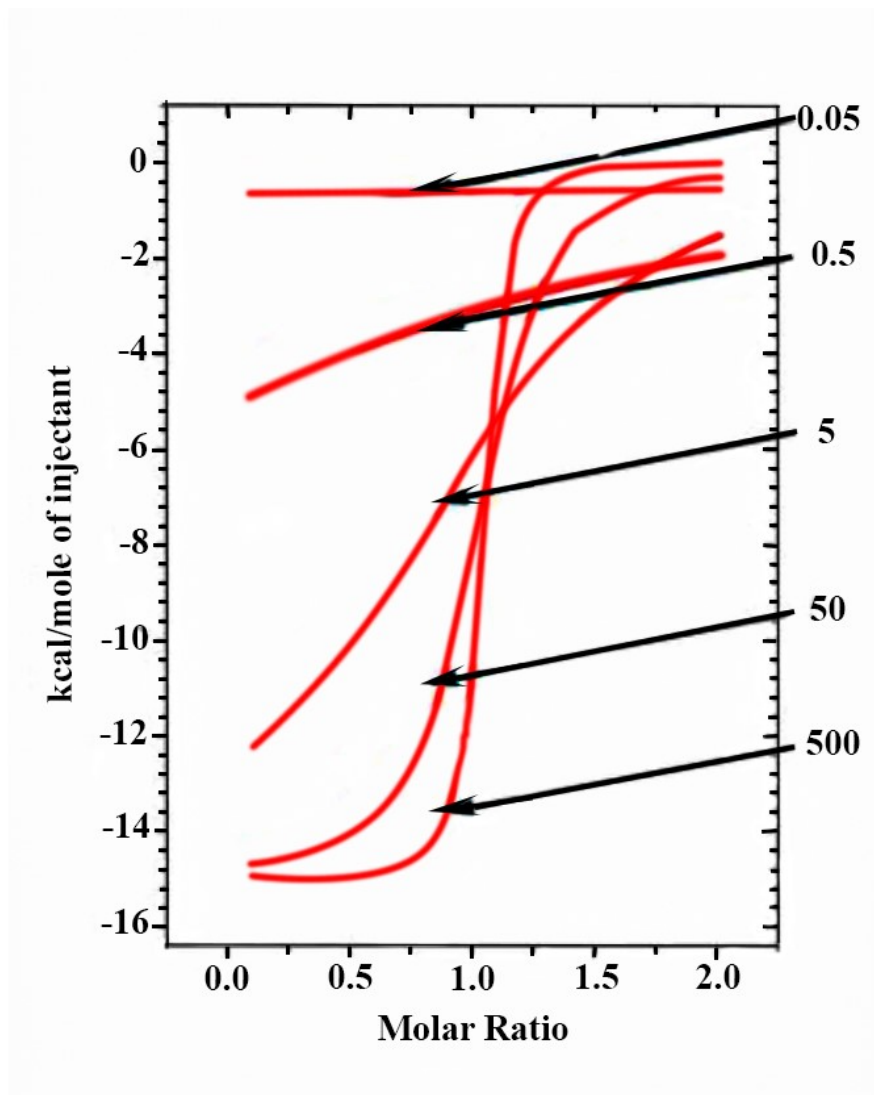


Figure 15. The examples of simulated curves at different c -values using the same ligand and titrant. In the simulated graph, the measured energy is plotted on the y -axis (kcal/mole of injection), while the x -axis is represented by a molar ratio (ligand/macromolecule). The figure was taken without modification.⁸⁹

Equation 1. Formula to calculate a c -value

$$c = n \cdot M_{tot} \cdot K_A$$

Where c -value is a theoretical affinity-related parameter, also known as a ratio between macromolecule and dissociation constant, n – binding stoichiometry, M_{tot} – molar concentration of ligand in the cell. K_A – association equilibrium constant.

Typically, for a 1:1 binding reaction when there is only one binding site, the concentration of titrant (here it is creatinine) should be 10-20 times higher than the concentration of the molecule in the cell (aptamer).⁸⁹ The molecule in the cell should be saturated or be so close to being saturated by the end of the titration.

According to our computational simulations and calculations (Eq. 1), aptamer should be added to the cell as a big molecule at a concentration of 100 μM , and the syringe should be filled with 1500 μM of small molecule creatinine.⁸⁹ Both samples (titrant and ligand) were diluted in a buffer: HEPES (10 mM), NaCl (150 mM), KCl (5 mM), MgCl_2 (2 mM), pH = 7.5.⁷⁰ The experiment was performed with 16 injections at room temperature.

stranded DNA that can be attached to a gold surface of the electrode through the formation of the S-Au bond via the thiol group. The thiol group can be chemically attached to the DNA sequence in 3' (see sections 2.3.1 and 2.5.2).^{63, 90, 91} Additionally, we mimicked the capturing strand from the selection strategy (here sigDNA) in the electrochemical strategy, labelling this strand with methylene blue redox element responsible for electron shuttling. (see section 2.5.3). In my designed strategy, the sigDNA is complementary to the capDNA. However, at the same time, the sigDNA is complementary to the aptamer too. Keeping in mind that the aptamer can specifically bind to an analyte and change its conformation, as discussed previously (see Chapter 1, section 1.3.2.3), we designed the following mechanism.

The first step in fabricating our sensor is to immobilize the capDNA (concentration of 3 μ M) onto the gold surface.⁹² The preformed duplex between the aptamer (concentration of 300 nM) and the sigDNA (concentration of 100 nM, strand with a redox element, see section 5.3) is added to the gold electrode. The incubation time of the duplex was 10 min at room temperature in a dark place to prevent the degradation of the light-sensitive redox element. This step helps to imitate a part of the selection procedure since the aptamer has been selected using a ratio of 1:3 (one part of the aptamer and three parts of its complementary strand). The idea is that the formed duplex between the aptamer and the sigDNA (two strands stay intact together) has a reduced electrochemical signal because only a few sigDNA strands are able to reach the electrode surface and hybridize with the capDNA (Fig. 16B *top*). Due to the folding of aptamer in the presence of the molecule of interest (for example, 0.5 mM of creatinine), the aptamer is released from its complementary strand sigDNA with methylene blue, and the duplex dissociates, thus releasing the sigDNA that now fully hybridizes with the capDNA (designed strand complementary to sigDNA) on the electrode surface. This produces a high electrochemical signal by having the redox-label strand with methylene blue close to the electrosurface (Fig. 16B *bottom*).⁹³

2.3. Design and Synthesis of DNA strands

2.3.1. Sequences of DNA-based sensor

The DNA strands used in this work are presented in the table below (Table 3). The sequences are listed from 5' to 3'.

Table 3. Sequences of designed DNA strands.

Name of the sequence	DNA sequence (5'-3')	Length	Base pair composition, GC content %	Melting temperature
Capturing DNA	C TCT CGG GAC GAC-SH	13	69.2 %	54.9 °C
Signalling DNA (13)	Methylene blue-GTC GTC CCG AGA G	13	69.2 %	54.9 °C
Aptamer A) Original	CTCTCGG GAC GAC(N40Confidential) G GGG TGT CGT CCC	66	50 %	77.9 °C
Aptamer B)	CGAC (N40Confidential) G GGG TGT CGT	54	44.4 %	75.5 °C
Aptamer C)	(N40Confidential) GGG GT	45	40 %	72.3 °C
Aptamer D)	(N34Confidential) GG	36	34.2 %	66.9 °C
Capturing strand with BHQ	BHQ-GTC GTC CCG AGA G	13	69.2 %	54.9 °C
Capturing strand with BHQ	BHQ-GTT CTA TTC TTC A	13	30.8 %	38.4 °C

for aptamer with internal FAM				
Aptamer with FAM label	FAM- CTCTCGGGACGAC(N40Confidential) GGGGTGTCGTCCC	66	50 %	77.9 °C
Aptamer with internal FAM	CTCTCGGGACGAC(N40_T- FAM _Confidential) GGGGTGTCGTCCC	66	50 %	77.9 °C
Signalling DNA (11)	Methylene blue - C GTC CCG AGA G	11	72.7 %	49.3 °C
Signalling DNA (14)	Methylene blue - C GTC GTC CCG AGA G	14	71.4 %	58.9 °C
Moxi aptamer	Confidential	43	Unknown	Unknown
Capturing DNA_Moxi	TGA GGC TCG ATC-SH	12	58.3 %	49.5 °C
Signalling DNA_Moxi	Methylene blue -GAT CGA GCC TCA	12	58.3 %	49.5 °C

2.3.2. Synthesis of all designed strands

The designed DNA strands (labelled and unlabelled) were synthesized using a H-6 DNA/RNA Synthesizer from K&A Laborgeraete, Schaafheim. The strands were made by solid-phase chemistry using different phosphoramidites (Biosearch Technologies). All syntheses were performed on a 1 μ mol scale using CPG (Controlled Pore Glass) solid – support (Glenresearch). Following synthesis, unlabelled strands, including thiol modifications, were then deprotected with 1 mL of 30 % aqueous ammonium hydroxide for 16 hours at 55 °C. The strands with methylene blue were deprotected for 48 hours at room temperature in a dark place to prevent its degradation since methylene blue is light-sensitive. Depending on the modifications, the DNA strands were then purified either by reverse-phase cartridge (RPC) or by high-performance liquid chromatography (HPLC).

2.3.3. Purification of DNA strands by Reverse Phase Cartridge

Unlabelled DNA strands and strands containing the thiol group or the 'Black Hole Quencher[®]-1' (BHQ-1) modifications were purified by RPC, because these strands have a 5' hydrophobic protecting group (4,4'-dimethoxytrityl, DMT) that enables the strands to be retained by the hydrophobic resin of the cartridge. RPC purifications were performed with MicroPure II columns (BioSearch) according to the standard K&A Laborgerete's protocol using a P-8 purifier from K&A Laborgerete, Schaafheim.

2.3.4. Purification of labelled DNA strands by HPLC

DNA strands synthesized without a 5' DMT protecting group (i.e., strands containing 5'-methylene blue or 5' - fluorescein (FAM)) were purified using high-performance liquid chromatography (HPLC), a 1260 Infinity Quaternary LC System from Agilent Technologies. The two mobile phases were used: 0.1 M triethylamine pH=7.2 (TEAA) and HPLC grade acetonitrile (ACN) with the following elution gradient of 5-100 % over 21 minutes. The stationary phase was an XBridge Oligonucleotide BEH C18 OBD Prep Column, 130 Å, 2.5 μ m, 10 mm \times 50 mm from Waters Corporation. The labelled strands with methylene blue and FAM were detected using a standard diode-array detector monitoring two absorbances: 260 nm (DNA), 665 nm (methylene blue), and 520 nm (FAM).

2.3.5. Quantification of DNA strands

All DNA strands were quantified by absorption spectroscopy using a Nanodrop 2000c Spectrophotometer from Thermo Scientific. All synthesized strands were diluted in deionized water, and 1.5 μL of the samples were used. The concentrations of all DNA strands were calculated using the Beer-Lambert Law (Eq. 2):

Equation 2. The Beer-Lambert equation

$$A = \varepsilon \cdot c \cdot l$$

Where A is the absorbance measured with Nanodrop 2000c, ε is the molar absorption coefficient ($\text{M}^{-1} \text{cm}^{-1}$; for unlabelled DNA - ε depends on the DNA strand composition and can be estimated from the *Integrated DNA Technologies OligoAnalyzer Tool*. For labelled DNA the molar absorption coefficients of methylene blue- and FAM-labelled DNA are 65000 $\text{M}^{-1} \text{cm}^{-1}$ and 75000 $\text{M}^{-1} \text{cm}^{-1}$ respectively, c is the molar concentration (M), and l is the optical path length (0.1 cm). DNA has an absorption maximum at 260 nm. The labelled DNA strand with a redox moiety like methylene blue gives a shifted peak around 665 nm. Another peak of the labelled DNA with a FAM moiety would be at nearly 520 nm. All DNA strands were prepared as 100 μL of 100 μM stock solutions and stored at $-20\text{ }^{\circ}\text{C}$.

2.4. Fluorescent experiments

Fluorescence spectroscopy was performed with a Cary Eclipse Fluorescence Spectrophotometer from Agilent Technologies. All measurements were done in quartz cuvettes. The settings were: excitation (ex)/emission (em) slit widths of 5 nm, excitation of 498 nm and emission of 520 nm for FAM. All experiments were done at room temperature. Firstly, the aptamer with FAM label alone was recorded by adding 1.2 μL (final concentration 120 nM) to 1 mL of buffer (see section 2.1.2), mixing by pipetting prior to transfer into a quartz cuvette. After 3 min, the duplex was formed in a solution at a 1:1.2 ratio (1 Quencher and 1.2 Fluorophore) by adding 1 μL of the strand with BHQ-1 quencher to the previous solution. Binding with the molecule was initiated by gradually spiking 5 μL and 100 μL of 100 mM creatinine after 15 min when the equilibrium of the duplex was reached.

2.5. Electrochemical sensor

This section gives an overview of the electrode system, followed by an explanation of the functionalization procedure, choice of the redox element, characterization of the electrodes, and optimization of the electrochemical parameters.

2.5.1. Electrode system

Electrochemical measurements were performed using the 'Phase Zero Sensors' screen-printed electrodes from Conductive Technologies. These electrodes consist of a PET (polyethylene terephthalate) protective layer, a gold working electrode, a gold counter electrode, and a silver/silver chloride (Ag/AgCl) reference electrode with a screen-printed insulating dielectric (Fig. 17).⁹⁴ In principle, the working electrode is the electrode where the applied potential is controlled, and the current flow is measured. The potential is applied to the working electrode with respect to the reference electrode, which has a fixed and well-defined potential and no current passing through it. The counter electrode allows an electrochemical reaction to occur on its surface and transfer electrons. Consequently, in the three-electrode system, current flows from the working electrode to the counter electrode and the reference potential does not change.⁹⁵ The working electrode area has a diameter of 2 mm.⁹⁴ The required volume to cover the electrode system and perform the experiments is 65 μl .

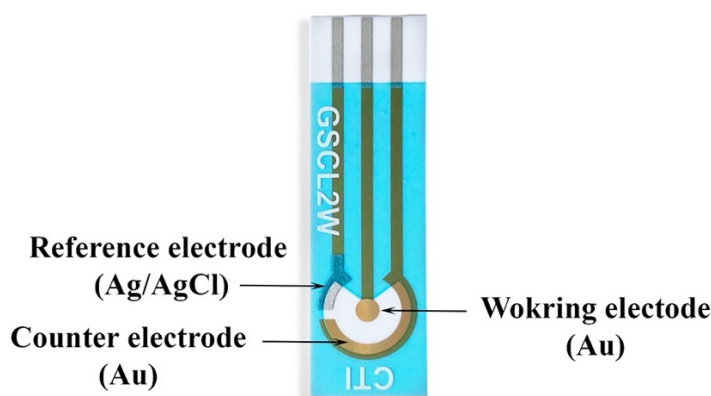


Figure 17. The screen-printed electrode 'Phase Zero Sensors'. Three electrode system: a working electrode (Au), a counter electrode (Au), and a reference electrode (Ag/AgCl). The figure was taken without modification.⁹⁴

2.5.2. DNA Immobilization onto the gold electrode surface

The first step is to obtain a reliably clean gold surface. The screen-printed CTI electrodes from Conductive Technologies were cleaned with 100 % isopropanol for 2 min by adding 65 μL to the working area. After the cleaning procedure, the electrodes were washed with deionized water, followed by drying with nitrogen (N_2) gas.

The electrochemical performance relies on the proper immobilization of DNA to the electrode surface. Among methods such as physical adsorption, linker-mediated coupling or bioaffinity interaction coupling, we chose chemisorption.⁹⁶ Surface functionalization was done according to the protocol of Keighley *et al.*⁹⁷ The protocol begins with the incubation of 4 μL of 10 mM TCEP (tris(2-carboxyethyl) phosphine) and 2 μL of 100 μM capDNA for 1 h in a small Eppendorf tube. TCEP reagent cleaves the S-S bond of the capDNA into 6-Mercapto-1-hexanol (MCH is a short-chain alkanethiol molecule) and 3'-SH-DNA (Fig. 18A). After 1 h of this reduction reaction, the buffer was added to dilute the mixture to the final concentration of capDNA of 3 μM (Fig. 18B). Then 5 μL of 3 μM reduced constructs was loaded to the working electrode surface (Fig. 18C).⁹³ All the electrodes were incubated overnight at 4 $^\circ\text{C}$ to attach capDNA and to form a self-assembled monolayer (SAM) on the gold surface (Eq. 3). Later, the electrodes were rinsed with DI water again.

Equation 3. The chemical reaction for the immobilization of capturing DNA on the gold surface



To obtain a well-formed Au-S-DNA/MCH layer, the electrodes were treated a second time with 5 μL of 2 mM of 6-Mercapto-1-hexanol (MCH) for 2 hours to remove loosely bound DNA and form a stable self-assembled monolayer. After passivation, the gold electrodes were again rinsed with DI water, followed by drying with N_2 gas.

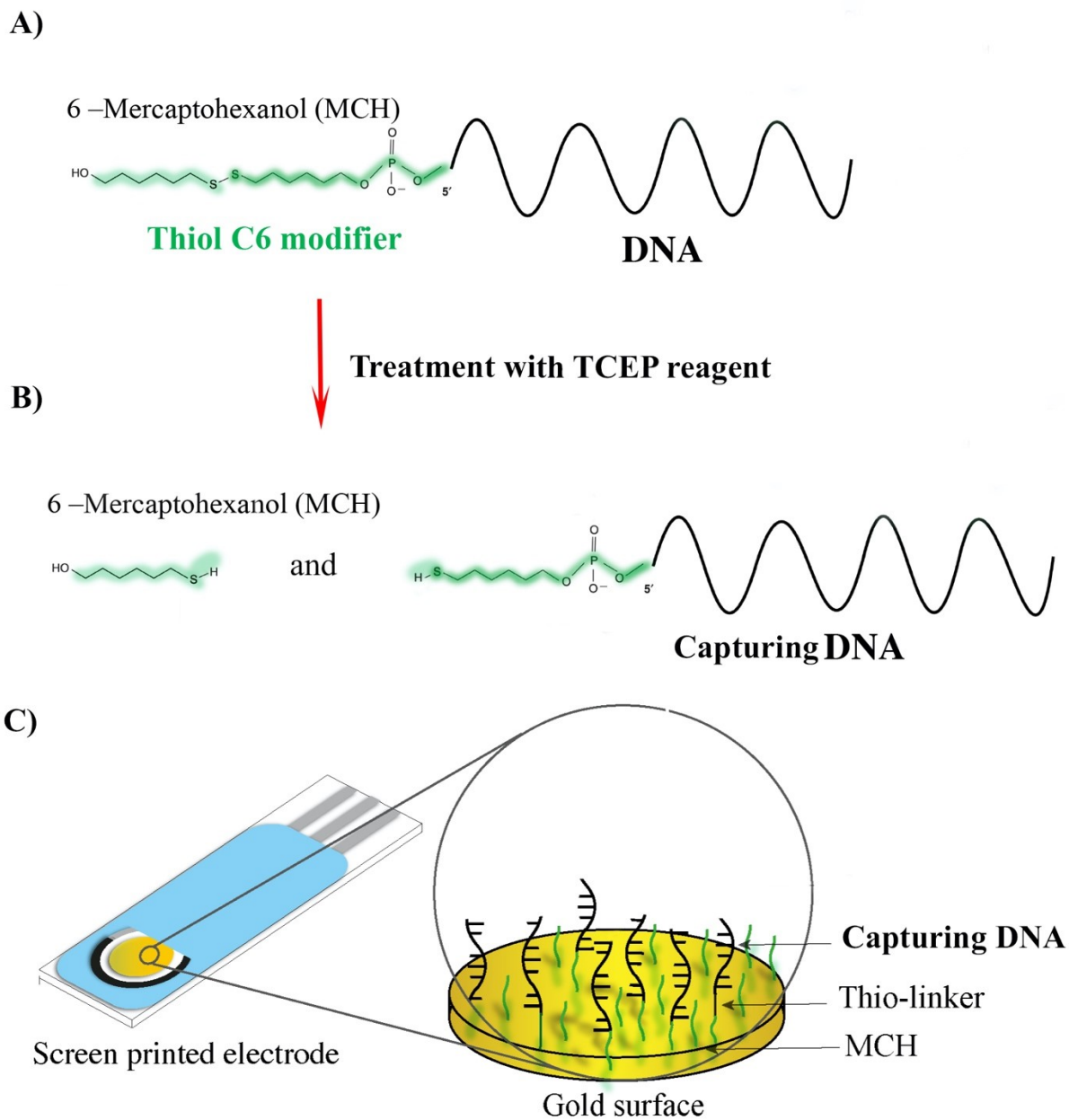


Figure 18. Schematic design of the capDNA and its immobilization onto the gold electrode surface. A) Structure of the synthesized capDNA strand. B) Treatment with a reducing reagent (TCEP). C) Immobilization of the capDNA onto the gold working electrode followed by MCH passivation.

2.5.3. Redox element

Over the past decade, methylene blue has been a redox element of choice to generate the electrochemical readout signal in E-AB-sensors. It is well-suited for electrochemical sensors because MB provides an efficient electron transfer (2 electrons during the redox reaction), good sensitivity, and strong stability at the negative potential window (Fig. 19A).⁹⁸ We covalently attached this redox element to a DNA strand to design a signalling strand (sigDNA) that will produce an electrochemical signal (Fig. 19B).

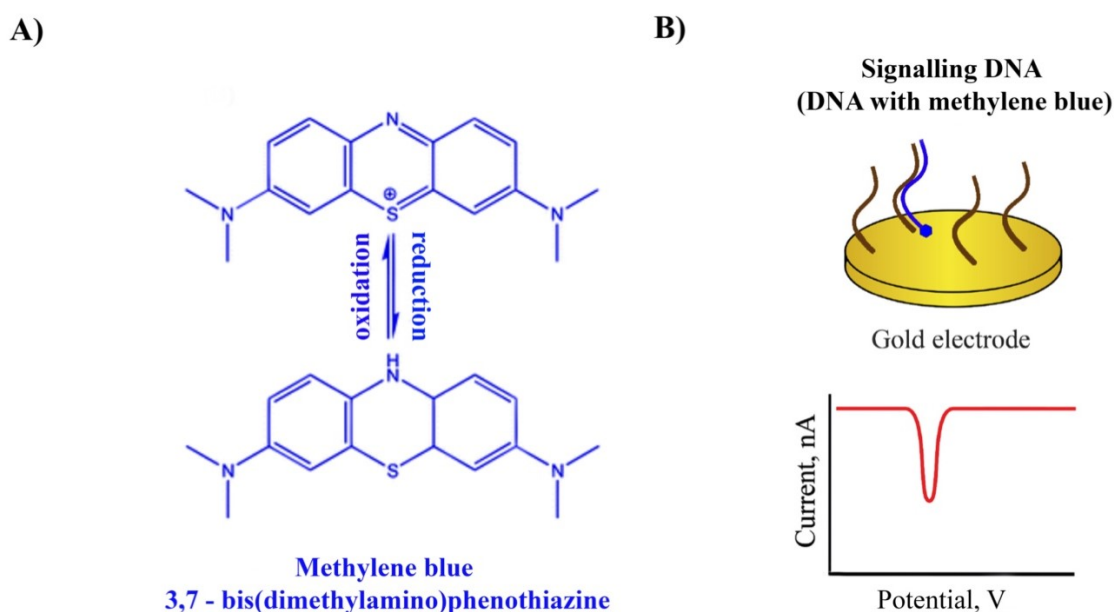


Figure 19. Redox element – methylene blue. A) Chemical structures of methylene blue. The figure was taken without modification.⁹⁹ B) *Top*: A sigDNA strand containing methylene blue hybridizes on the electrode surface with the immobilized capDNA strand. *Bottom*: The electrochemical response of methylene blue and voltammogram of the expected peak reduction.

2.5.4. Square wave voltammetry

Square wave voltammetry (SWV) is a form of pulse voltammetric technique that detects a change in current with great sensitivity. The current is sampled twice, just before the end of the forward-going pulse (point i_1) and at the end of the reverse pulse (point i_2) at the constant frequency.⁹⁵ The difference between the two sampled currents is plotted versus the applied staircase potential, as shown in Fig. 20. It is also a method of choice that has seen widespread adoption in the community due to its ability to discriminate between charging and faradaic currents and therefore achieve better sensitivity.⁵⁸

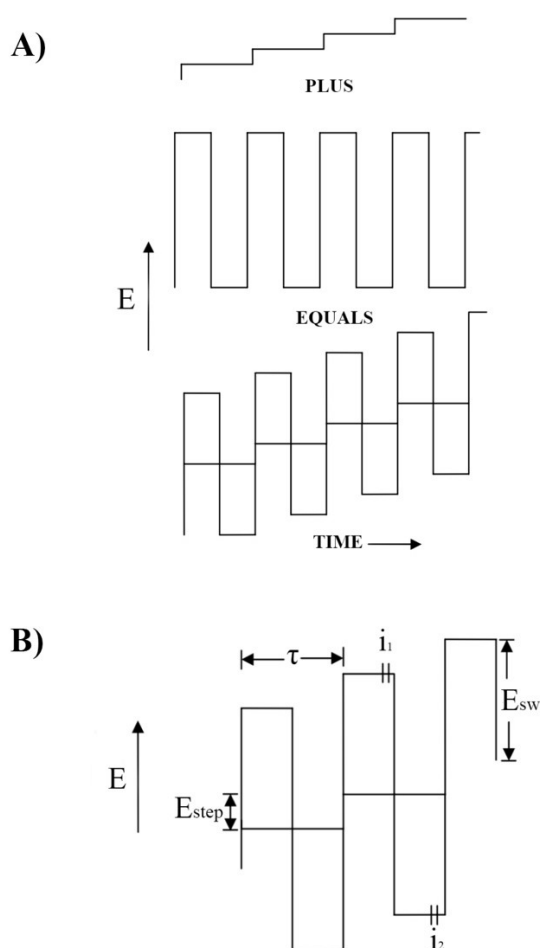


Figure 20. Square wave voltammetry overview. A) The waveform of square wave voltammetry combines staircase potential and square wave potential. B) The difference in currents sampled between point i_1 and point i_2 against applied potential. The figure was taken without modification.¹⁰⁰

In this work, SWV was used to determine the variation of electrochemical response in the presence of an analyte. Different creatinine concentrations were added to samples to obtain a binding curve. The electrochemical measurements were done at room temperature using square wave voltammetry from -0.10 V to -0.55 V (vs. Ag/AgCl) to record the reduction peak of methylene blue, with an amplitude of 25 mV and an optimal frequency of 90 Hz for 150 cycles. All peaks were extracted in the PSTrace software (of Palmsens Instrument) and drawn in KaleidaGraph graphing program.

2.5.5. Optimal frequency for electron transfer

Often the electrochemical response can be improved by tuning the frequency of the electrochemical method. The optimal frequency corresponds to the frequency at which the electron transfer is the most efficient. Therefore, the optimal frequency represents the maximal transferred charge and can be tuned by changing the frequency of the electrochemical method. To determine the optional frequency, we used SWV measurements.⁵⁸ To do so, the SWV was run in a range from -0.55 V to -0.15 V (vs. Ag/AgCl), using a 0.001 V step, a 100 mV/s scan rate, a 0.025 V amplitude, and frequencies ranging from 2 Hz to 750 Hz. After all measurements, we drew a Lovric Graph to find the optimal frequency for electron transfer (Fig. 21). For this assay, we determined that the maximum cumulative charge (top of the peak height) would be at a frequency of 90 Hz.

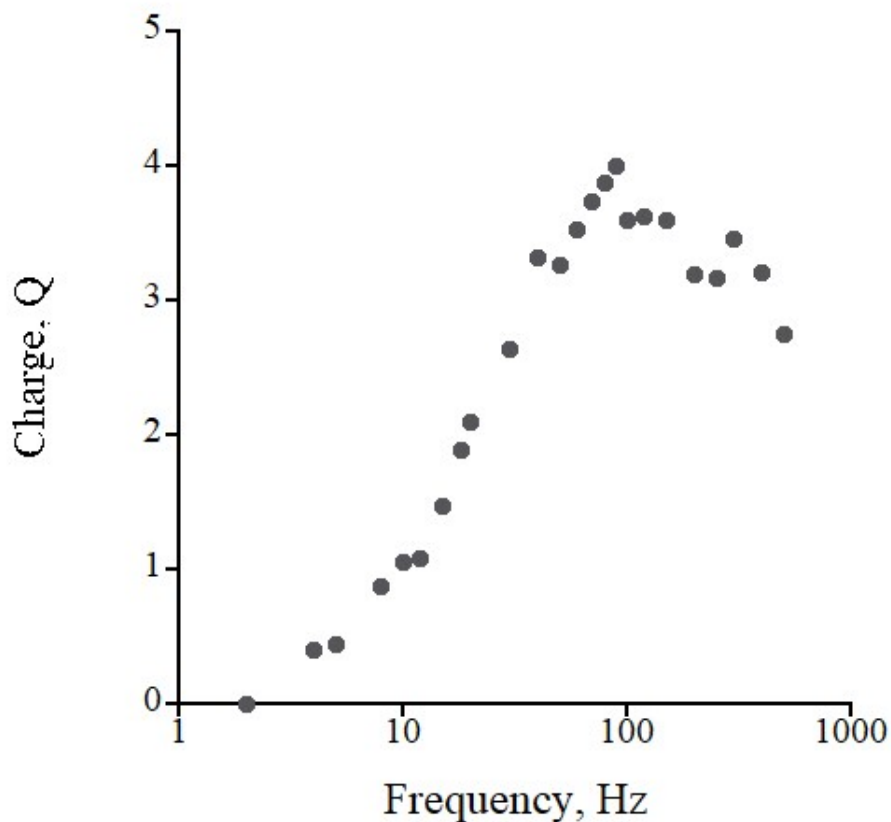


Figure 21. Lovric Graph shows the dependence of cumulative charge and frequency. Optimal frequency represents the maximum transferred charge.

2.5.6. Calculation of signal enhancement (signal gain)

The signal gain was calculated based on the definition of signal enhancement.¹⁰¹ Signal enhancement represents the difference between the peak current after adding the analyte and subtracting the initial peak current (without the analyte) divided by the initial peak current (Eq. 4).

Equation 4. The formula for the calculation of the signal gain

$$\text{Signal gain (\%)} = \frac{I_{\text{with analyte}} - I_{\text{without analyte}}}{I_{\text{without analyte}}} \cdot 100 \%$$

2.6. Sensor characterization

The performance of a biosensor can be evaluated using four analytical parameters: sensitivity, specificity, experimental reproducibility, and dynamic range. These parameters will help to develop an effective biosensing architecture for future point-of-care devices. The sensitivity is defined as the ability of the sensor to respond reliably and quantitatively to changes in different analyte concentrations. Usually, sensitivity is closely associated with the limit of detection (LOD), and the LOD is the lowest concentration of an analyte that can be reliably detected with stated confidence.¹⁰² The sensitivity can be determined by the concentration variation in the electrochemical measurements; it is defined as the slope of the linear response. However, in our work, this characterization step is still ongoing and needs more time to be completed (the results are not shown). The specificity was defined as the ability of the sensor to distinguish the analyte from other molecules in the sample.¹⁰² The specificity of this biosensor was tested by comparing the heat response measured by the ITC instrument in the presence of urea. We choose this molecule as a model because it has a similar chemical structure to creatinine. The instrument and intra-assay precisions were done during my research work. The instrument precision means that the same sample with the same volume was repeatedly introduced into an instrument more than ten times. The intra-assay precision is defined by analyzing samples several times by one person on one day with the same instrument.¹⁰² The dynamic range was defined as the concentration range over which there is a measurable response.¹⁰² To identify the dynamic range, a binding curve was used to evaluate the sensor's

performance. Typically, the dynamic range is defined by the analyte concentration over which the sensor response ranges from 10 % to 90%. The electrochemical current is plotted on the y-axis, while different measured concentrations are plotted on the x-axis (log function). All experiments were repeated at least three times (n=3).

2.7. Sensor validation in serum

In order to determine the ability of the sensor to detect the specific target in its intended biological matrix, we validated our sensing mechanism in serum (ISERS50ML-36688-12, Innovative Research). For our preliminary results, we additionally spiked 1 mM of creatinine in serum with an unknown creatinine concentration. Keeping in mind that serum naturally contains creatinine, we needed to degrade the creatinine molecule in the sample prior to performing our measurements. To do so, for our negative control, we added an enzyme 'creatinine deiminase' (Creative-Enzymes, 10U/mg, 5KU, activity 1500 U/ml) to cleave creatinine into N-methylhydantoin and ammonia.¹⁰³ Using this enzyme for the negative control helped us to properly validate the designed sensing strategy in a complex sample and avoid false-positive results.

Chapter 3 – Results and Discussion

This chapter presented the characterization results of the creatinine aptamer. Two attempts to adapt this aptamer into an electrochemical sensor using already developed sensing strategies were reported: the “one-component assay” (see Chapter 1, section 1.3.2.3) and the “three-component assay” (see Chapter 1, section 1.3.2.4). As we will see, these attempts have not been successful. In response, we have engineered and tested a novel signalling mechanism inspired by the selection procedure employed for the creatinine aptamer selection. To begin with, we designed and tested this strategy using fluorescence spectroscopy. Then, we adapted the fluorescence signalling mechanism into an electrochemical signalling mechanism. This signalling mechanism was further characterized, optimized, and validated in a complex biological medium such as serum. The potential universality of our proposed sensing mechanism was further suggested by adapting a commercially available aptamer to detect the Moxifloxacin antibiotic.

3.1. Characterization of the creatinine aptamer

The aptamer is the key recognition element responsible for selectively detecting the target. Finding an aptamer for detecting small molecules has been shown to be challenging.⁷⁴ We have the aptamers that have been selected for creatinine binding and that have a length of 66 nt, which is above the average length of aptamers. Usually, the length of aptamers is typically between 25 and 50 nt.¹⁰⁴⁻¹⁰⁷ We first analyzed the potential fold of the one aptamer (see Chapter 2, section 2) using *UNAFold* to estimate its secondary structure, its stability, its melting temperature, and its GC content under our reaction conditions: 10mM HEPES, 150 mM NaCl, 5 mM KCl, 2 mM MgCl₂, and pH = 7.5, room temperature (Fig. 22A).^{70, 84} The predicted structure of the aptamer has a stable stem, three loops, and shows good stability (negative free energy of Gibbs -7.25 kcal) (Fig. 22B).

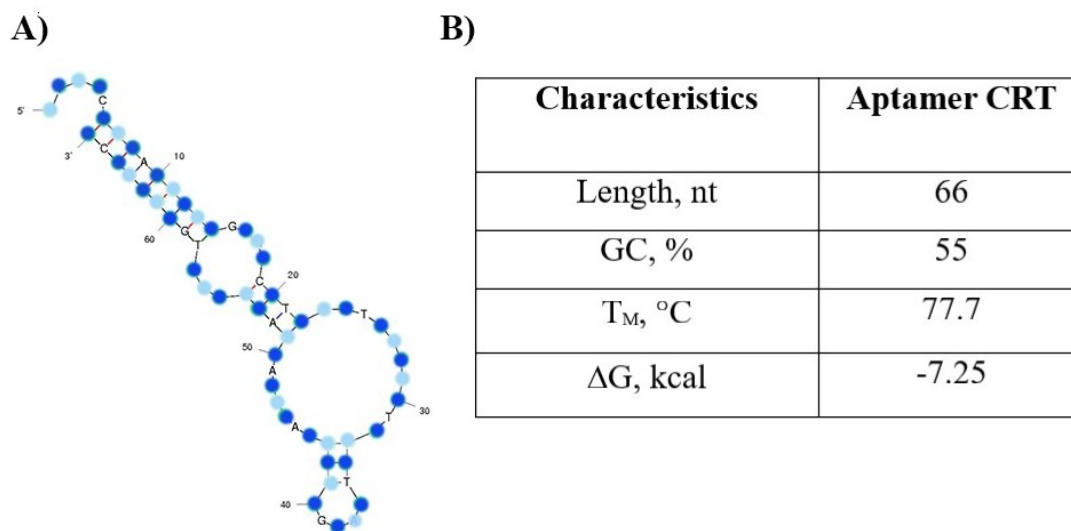


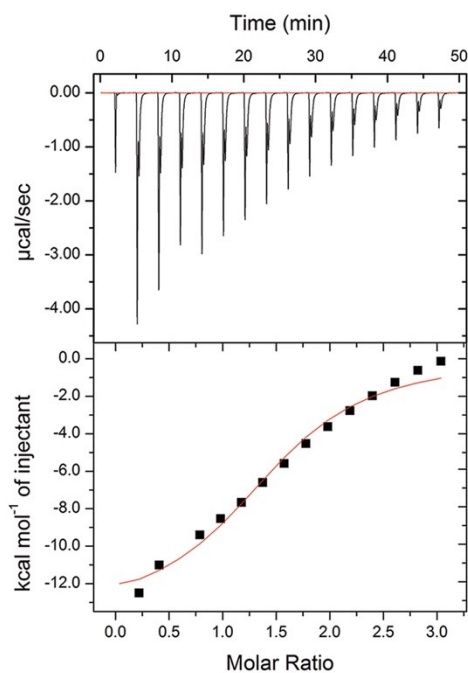
Figure 22. Characterization of the creatinine aptamer. A) The predicted secondary structure of the creatinine aptamer, and B) Its characteristics predicted by *UNAFold*. Of note, the complete sequence of the aptamer is not disclosed due to an ongoing non-disclosure agreement.

3.1.1. Characterization of the aptamer binding affinity

We then characterized the aptamer's binding affinity. We performed ITC experiments, which showed that the aptamer binds to creatinine with a calculated K_d value of 19 μM (Fig. 23A) (see Chapter 2, section 2.1.1 for the details of the calculations). We found that the binding of creatinine with the aptamer is driven by a negative change in enthalpy ($\Delta H = -13.6$ kcal/mol), indicating that it is an exothermic process. Also, we obtained $n = 1.3$, suggesting a single binding site. Interestingly, the calculated K_d value (19 μM) also corresponds to the clinically relevant ranges of creatinine (see Chapter 1, section 1.1; [equivalent to 53-106 μM]) suggesting that this aptamer may display an optimal sensing range.

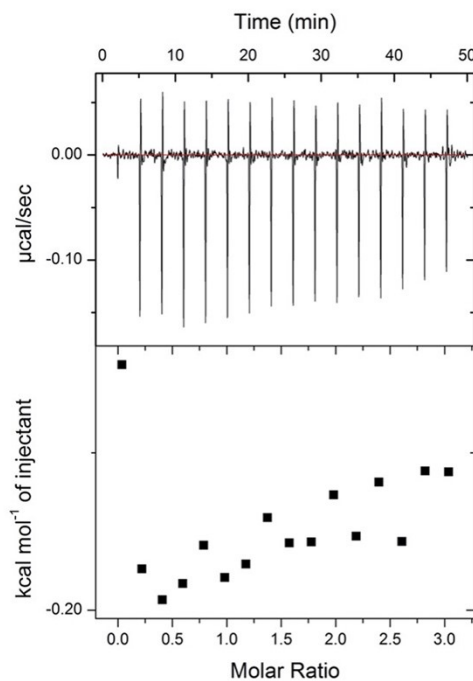
In order to explore the selectivity of the aptamer-creatinine interaction, we measured the binding affinity between the aptamer and urea. Urea and creatinine are two small molecules with similar chemical groups (e.g., amino groups), and since the normal urea concentration is around 100-fold higher than the creatinine concentration, potential interference is possible. We, therefore, ran an ITC experiment on urea and confirmed that no interaction was detected between the creatinine aptamer and urea (Fig. 23B).

A) Creatinine



$$K_d = 19 \mu\text{M}$$

B) Urea



No binding

Figure 23. ITC characterization of the creatinine aptamer. A) *Top*: raw data, and *Bottom*: binding isotherm of the aptamer with creatinine. B) *Top*: raw data, and *Bottom*: binding isotherm of the aptamer with urea.

3.1.2. Attempt at designing a shorter creatinine aptamer

After confirming that the aptamer selectively binds to its target, we explored whether we could further reduce the length of the aptamer. Indeed, long aptamers often display folding challenges.^{57, 75, 108} Knowing that the extremities of the aptamer are made of a DNA sequence designed for structure-switching mechanism, we decided to cut the extremities of the aptamer while verifying if the aptamer still retained its binding affinity. We found that deleting 4 WC bp in the stem and 5 nt in the tail to get a length of 54 nt enables to keep a K_d value of 54 μM versus 19 μM for the original aptamer wild type (Fig. 24B). The increase in K_d value (less than 3-fold) suggests that the deleted base pairs were contributing to the binding affinity of creatinine. In contrast, the 45 nt aptamer (- 8 WC bp and - 5 nt in the tail) (Fig. 24C), and the shortest 36 nt aptamer (removed 30 nt from the left side) (Fig. 24D) displayed no binding activity to creatinine. All these results confidently suggest that the whole length of the aptamer is important and should not be modified. Removing base pairs from the original aptamer can disrupt its binding site leading to low or no binding to the target. Given the smallest affinities of the shorter versions of the aptamer, we decided to keep the original 66 nt version for the adaptation into a sensor.

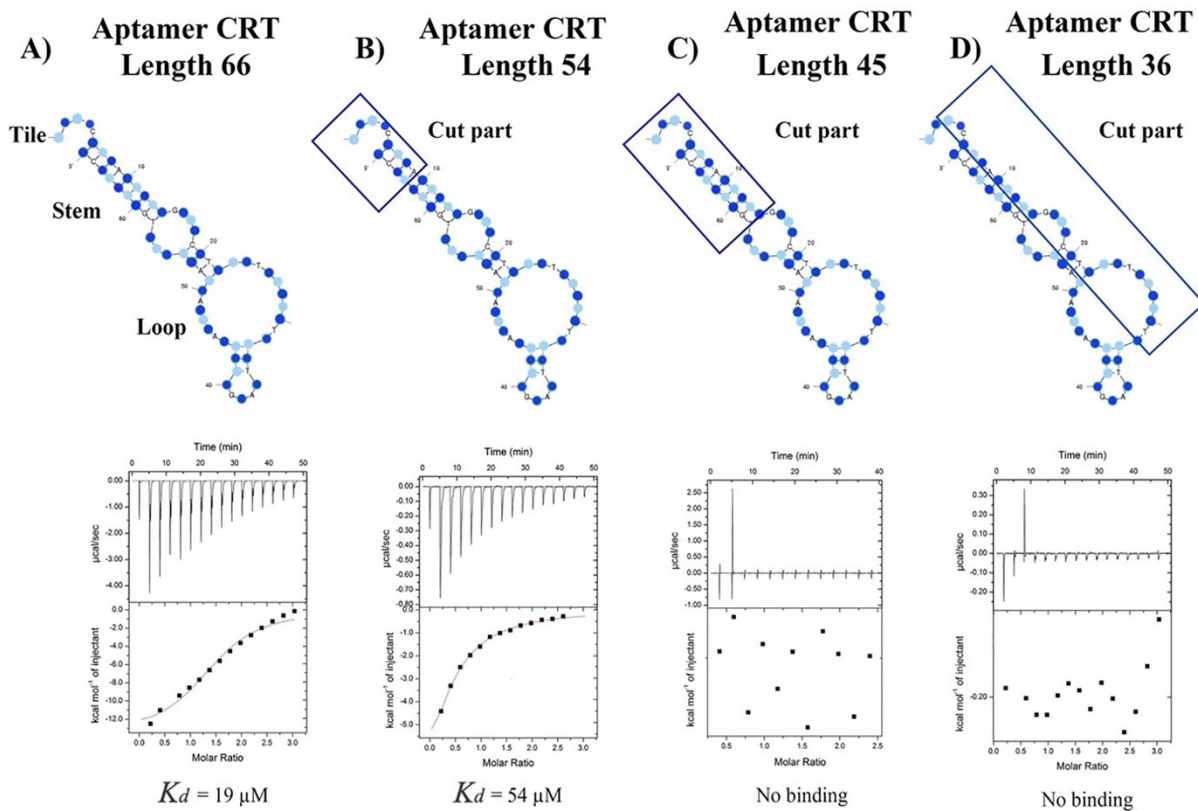


Figure 24. Reducing the length of the aptamer reduces its affinity for creatinine. The original aptamer length is 66 nt. We removed various sections (see *blue box*) to create shorter aptamers with lengths of 54 nt, 45 nt and 36 nt, and then determined their binding activities to creatinine.

3.2. Engineering signalling mechanisms

Many strategies have been explored to date to adapt aptamers into efficient electrochemical sensors.^{64, 106, 109-113} In this section, we first explored the integration of the creatinine aptamer into an E-AB sensor using the “one-component” and “three-component” assays. Because these two strategies failed, we developed a novel signalling mechanism based on the capture-SELEX procedure.

3.2.1. Classic electrochemical aptamer-based assays

3.2.1.1. One-component assay

The most popular signalling mechanism employed to adapt aptamers into electrochemical sensors consists of attaching the aptamer directly to the electrode via one of its extremities while adding a redox molecule to its other extremity. This “one-component” sensor (see Chapter 1, Section 1.3.2.3), pioneered and popularized by Prof. Plaxco, has already been tested on various creatinine aptamers.^{63, 64, 105} Indeed, Prof. Plaxco has confirmed with us that none of the creatinine aptamers worked in the well-known “one-component” assay. The reason behind this failure was not clear. Destabilizing mutations to optimize the folding-upon-binding mechanisms of these aptamers were also tried, but none of them produced working sensors.

3.2.1.2. Three-component assay

Motivated by recent successes obtained in our laboratory on a newly developed “three-component” aptamer-based signalling mechanism (see Chapter 1, section 1.3.3), we decided to test this approach with the creatinine aptamer. To do so, we designed the MB-labelled sigDNA that is complementary to the first 13 nt of the 5' end of the aptamer (Fig. 25A). We performed the assay, as reported, in a one-step manner by simultaneously adding all three components (the sigDNA, the aptamer, the capDNA-electrode) to the sample containing or not 0.5 mM of creatinine. The kinetic rate k_1 (between creatinine and the aptamer) is expected to be much faster than k_2 (kinetic rate between aptamer and sigDNA) and k_3 (kinetic rate between sigDNA and the capDNA).

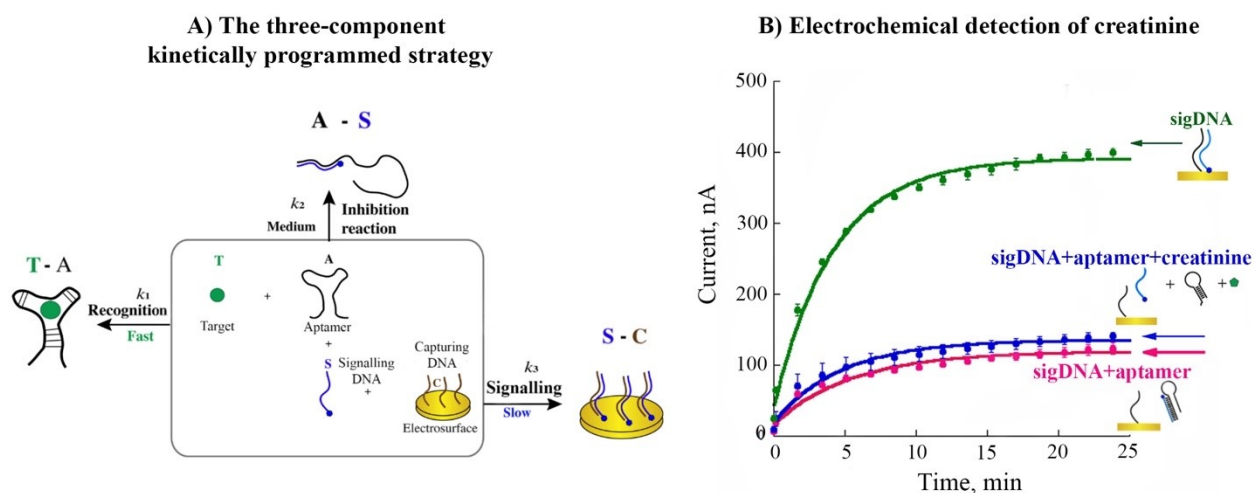


Figure 25. Adapting the creatinine aptamers into a “three-component” strategy failed. A) The schematic design of the kinetic assay. B) The electrochemical detection of creatinine. All three components were added together according to the “kinetically programmed strategy”. The data points are the average of triplicated measurements. The error bars, representing the standard deviations, are too small to be seen.

In the presence of high creatinine concentrations, we expected the aptamer to be sequestered in a conformation that precludes binding to the complementary sigDNA. In this case, the sigDNA containing methylene blue would be free to reach and hybridize the capDNA at the surface of the electrode, thus generating a large electrochemical current. Unfortunately, we did not observe a difference in signal between the sample containing creatinine (*blue data*) or not (*pink data*) (Fig. 25B). Although the sigDNA seems to be able to bind to the aptamer (see *pink data*: lower electrochemical signal in the presence of the aptamer), creatinine binding to the aptamer (*blue data*) does not appear to sequester the aptamer further and limit its ability to bind to the sigDNA. Unfortunately, these results also suggested that the “three-component” strategy is not universal either.

3.2.2. Signalling strategies based on SELEX

Over the years various groups employed a fluorescent strategy based on the SELEX strategy to characterize the affinity of their selected aptamers (see chapter 1, section 1.3.3).^{71, 79, 81} We therefore hypothesized that employing a similar strategy to create an electrochemical sensor may represent a universal signalling mechanism. We tested this idea by first employing a fluorescent signalling mechanism, which is simple in terms of performance.¹¹⁴ We then adopted a similar strategy for an electrochemical sensing assay.

3.2.2.1. Validating the signalling mechanism based on the selection strategy using fluorescence

A fluorescent assay provides a rapid and inexpensive strategy to characterize a signalling mechanism. We, therefore, employed this experiment to demonstrate that creatinine binding induces dissociation between a signalling DNA sequence (sigDNA or capturing strand from the selection) and the aptamer. To do so, we labelled the 5'-terminus of the aptamer with the FAM moiety and the 3'-terminus complementary strand (i.e., the sigDNA) with the BHQ-1 moiety that absorbs efficiently the wavelength emitted by FAM.¹¹⁵ In this experiment, if the sigDNA is released from the aptamer in the presence of creatinine, an increase in fluorescence should therefore be detected. We first noticed that the unbound aptamer produces a high fluorescent signal via its FAM moiety, with an intensity of around 180 a.u. (Fig. 26A). As expected, when adding the complementary strand (sigDNA) containing the BHQ-1, the fluorescence decreased by 86 %. We then spiked increasing amounts of creatinine (0.5 mM and 10 mM) and observed a simultaneous increase in the fluorescence signal (relatively 88 % and 172 %), confirming that creatinine induces the dissociation of the sigDNA from aptamer. This result suggests that the signalling mechanism is similar to the proposed structure-switching mechanism selected via the capture-SELEX strategy. It also demonstrates that it is likely adaptable to an electrochemical format since we can also label the releasing strand with a redox element.

While investigating this signalling mechanism, we also considered the effect of changing the binding location of the sigDNA in the aptamer-sigDNA complex. Since the selection strategy was not performed using this specific aptamer duplex, we hypothesized that creatinine addition

might not be able to release the signalling strand. We, therefore, labelled the aptamer with an internal Fluorescein moiety (FAM attached to thymine) that matches the location of the new complementary signalling DNA (Fig. 26B). When the aptamer was alone, the FAM produced a high fluorescence signal (near 100 a.u.), and once hybridized to its quencher-labelled complementary strand we observed a slow (around 15 min) signal decrease by up to 80%. However, no increase in fluorescence signal was observed upon the addition of 0.5 mM and even 10 mM creatinine, suggesting that creatinine is not able to displace the sigDNA from the aptamer. It is therefore unlikely that this specific signalling mechanism will work in an electrochemical format. Overall, these results confirm that the selection process involved in the capture-SELEX has already optimized a signalling mechanism that triggers the dissociation of a capturing strand from the selection (here the sigDNA) upon binding to the target (creatinine), which can be readily adaptable into an electrochemical format.

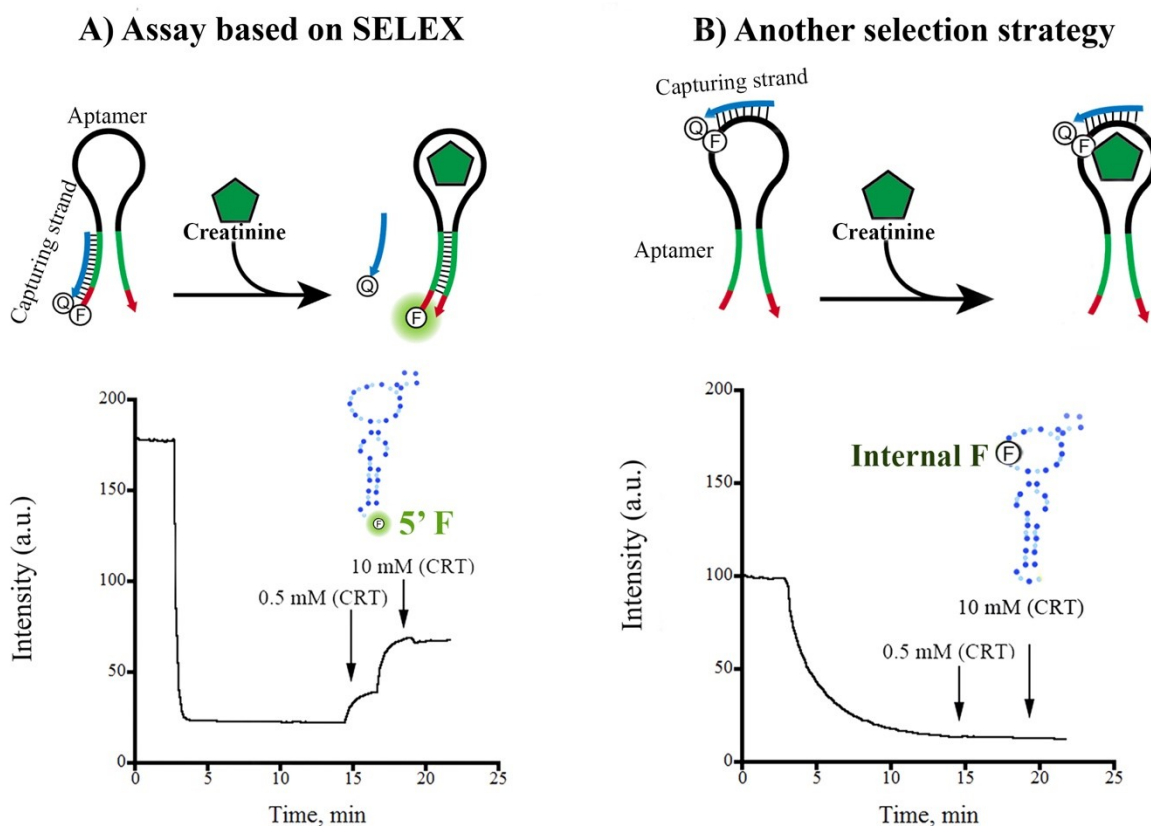


Figure 26. The importance of the sigDNA location in fluorescent assays. A) The schematic representation of the aptamer and the capturing strand from the selection. Fluorescence data

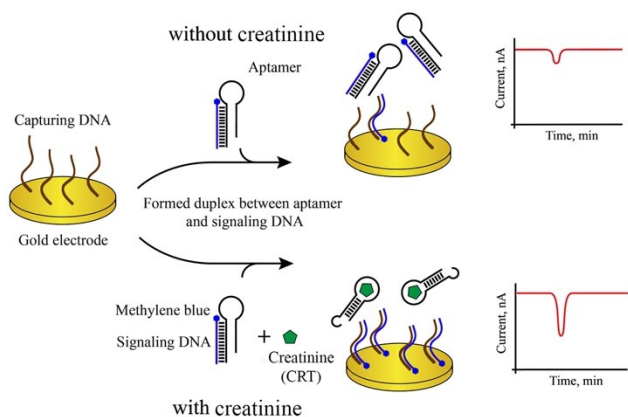
shows that, in the presence of creatinine, the sigDNA dissociates from the aptamer, thus generating a fluorescent signal. B) Fluorescent imitation of the assay based on another strategy. The sigDNA decreases fluorescence upon adding creatinine; no fluorescent signal was observed.

3.2.3. Adapting the signalling mechanism into an electrochemical format

3.2.3.1. Design and validation

The SELEX-based signalling mechanism releases a short DNA strand. Thus, we decided to label the released strand with the redox element methylene blue so that it could be easily detected following hybridization with its complementary DNA strand attached to an electrode (Fig. 27A; see more details in Chapter 2, section 2.2 and 2.5.2). We then hybridized this released strand, now called sigDNA, to its aptamer and added this DNA duplex to a sample containing, or not, creatinine. In the absence of creatinine, we found that the sigDNA remains relatively sequestered by the aptamer and does not hybridize efficiently with its complementary DNA strand on the surface of an electrode (Fig. 27B, *pink*). In contrast, in the presence of creatinine, the sigDNA dissociates from the aptamer and produces a higher electrochemical current (Fig. 27B, *blue*). More specifically, when employing 100 nM of sigDNA and three times more aptamer (300 nM), a signal gain of 55% (equation 4) is observed in the presence of 0.5 mM creatinine after 15 min (Fig. 26B).

A) The strategy based on the selection procedure



B) Electrochemical detection of creatinine

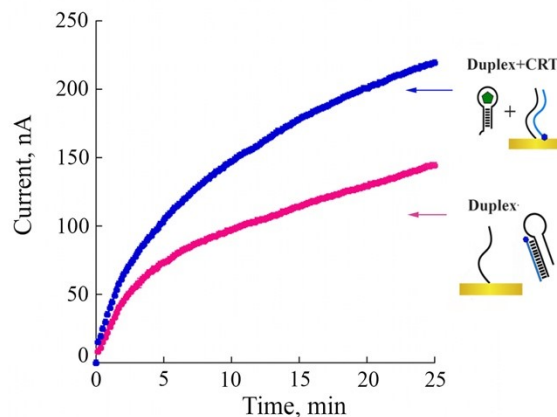


Figure 27. Electrochemical adaptation of the signalling mechanism. A) A schematic representation of the signalling mechanism based on the selection procedure. *Top*: without creatinine, and *Bottom*: with creatinine. B) Electrochemical detection of creatinine. *Pink*: without creatinine, and *Blue*: with creatinine. The signal gain in the presence of 0.5 mM creatinine was 55% after 15 min. The data points are the average of triplicated experiments. The error bars, representing the standard deviations, are too small to be seen.

3.2.3.2. Optimizing the sigDNA:aptamer ratio

A 55% signal increase in the presence of 0.5 mM creatinine is a good starting point for sensor development. To further improve the signal gain of this sensor, we decided to explore different sigDNA:aptamer ratios (from 1:1 to 1:4). We hypothesized that increasing the aptamer concentration relative to the sigDNA may enhance the signal gain by reducing the signal background in the absence of creatinine (i.e., more sigDNA in complex with the aptamer) (Fig. 28). As predicted, we found that increasing the concentration of aptamer (e.g., 1:2 and 1:3) decreases the signal background and improves the signal gain by approximately 50 %. However, adding too much aptamer (1:4) seems to reduce the efficiency of sigDNA dissociation drastically. This is likely attributable to the increased energetic cost related to dissociating the sigDNA from the aptamer in the presence of high concentrations of aptamer, which drives the equilibrium toward DNA duplex formation. These results confirmed our hypothesis that the signal gain might be improved by changing the ratio between sigDNA:aptamer. Interestingly, the ratio (1:3) that was used in the selection procedure was also found to be optimal for generating the higher signal gain. It is the only case in which an unexpected increase in the signal gain is observed 3 min after beginning the reaction (Fig. 28C). This can be explained by the strong interaction between the sigDNA and the aptamer in solution (decrease in signal gain) followed by the dissociation of the two strands on the electrode surface in the presence of creatinine (increase in signal gain).

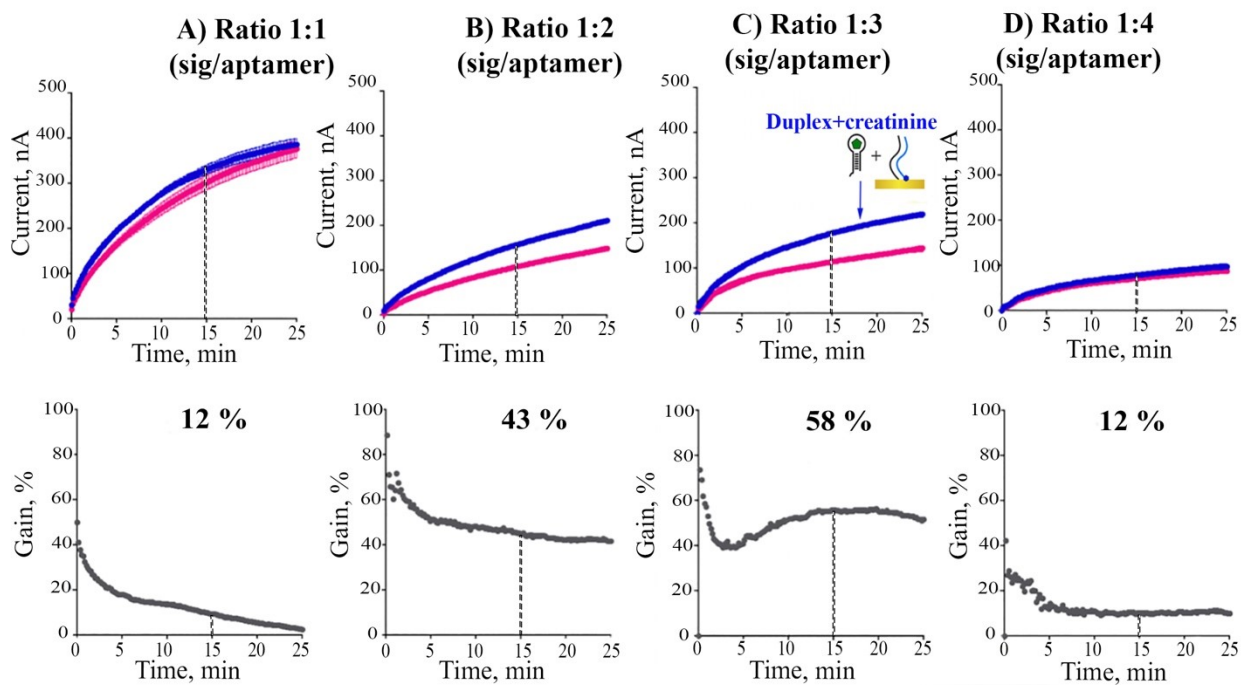


Figure 28. Optimizing the signal gain by exploring different sigDNA:aptamer ratios (from 1:1 to 1:4). The data points are the average of triplicated experiments. The error bars, representing the standard deviations, are too small to be seen.

3.2.3.3. Other strategies to improve a signal gain

In order to improve the signal gain of the sensor, we further explored the effect of varying the affinity between the aptamer and the sigDNA.¹¹⁶ A higher affinity aptamer-sigDNA duplex should lead to a smaller background signal in the absence of creatinine, but it should also require more energy (i.e., more creatinine should be added) to enable duplex dissociation.¹¹⁷ To identify the optimal aptamer-sigDNA affinity, we designed complementary sigDNA with lengths varying from 11 to 14 nt (Fig. 29). We found that the lower affinity duplex displayed a similar gain to the original length (13 nt) (58% vs 55% after 15 min) despite showing a higher background. In contrast, the higher affinity duplex (with the longer sigDNA 14 bp) increased the gain of the assay up to 75% via a reduced background signal. This result confirmed that a stronger aptamer-sigDNA complex enabled the sequestration of more sigDNA, thus reducing the background while still allowing sufficient dissociation in the presence of an intermediate concentration of creatinine (0.5 mM). Interestingly, the similar curve trends were observed with sigDNA 13 and 14 nucleotides in less than 3 min (Fig. 29 B and C). These results suggest that forming a more stable duplex between the sigDNA-aptamer affects the duplex association/dissociation occurring on the electrode surface.

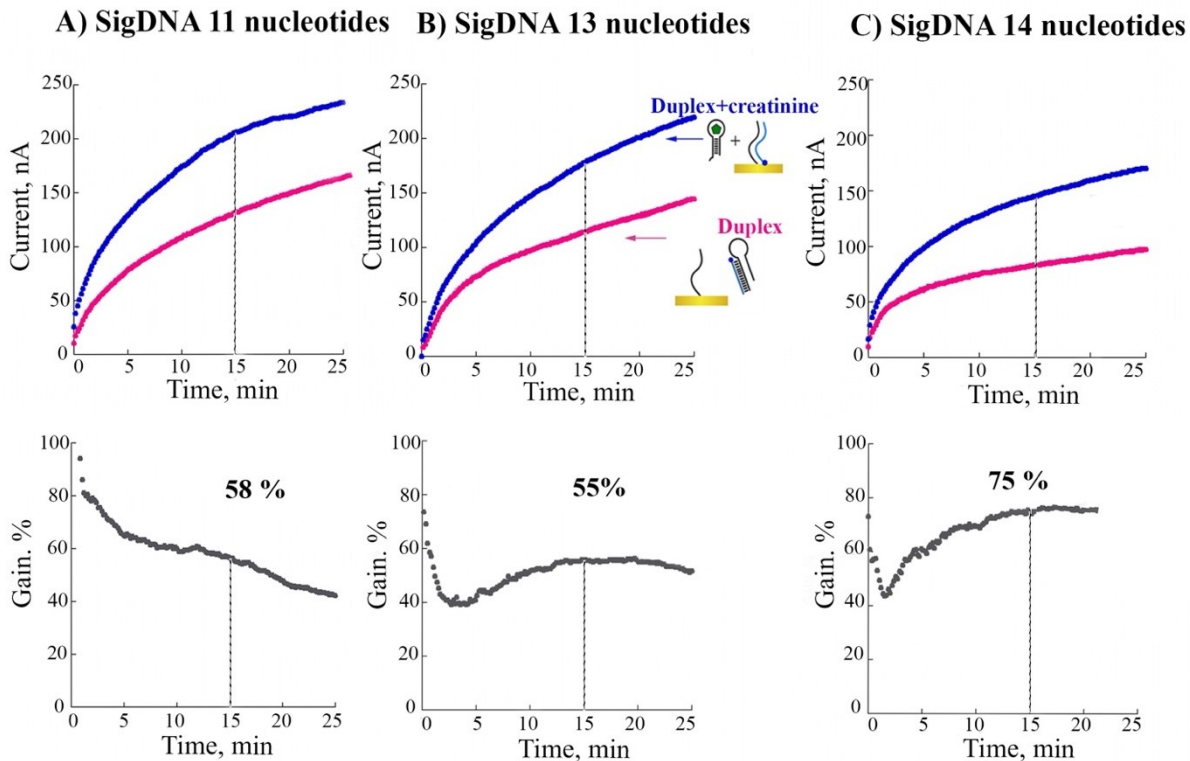


Figure 29. Increasing the hybridization length and affinity of the sigDNA for the aptamer reduces background signal and improves signal gain. The data points are the average of triplicated experiments. The error bars, representing the standard deviations, are too small to be seen.

3.2.3.4. Determinating the dynamic range of the sensor

A practical creatinine sensor needs to be precise between 27 μM and 1056 μM , which corresponds to the typical range of creatinine concentration measured in human blood (Chapter 1, section 1.1).¹¹⁸ However, the normal creatinine concentration in whole blood typically ranges from 50 μM to 100 μM ; higher concentrations are considered abnormal. The aptamer employed in this study possesses a K_d of 19 μM (see Chapter 3, section 3.1), which suggests that the optimal sensitivity of the sensor should be between 2.1 μM and 171 μM (i.e., a typical 81-fold between 10% and 90% signal).¹¹⁹ To determine whether our engineered signalling mechanism has an effect on the dynamic range of the creatinine aptamer, we performed a binding curve by spiking different concentrations of creatinine in buffer (from 30 μM to 1 mM). By doing so, we obtained a significantly more cooperative binding curve that did not fit well with the classic binding isotherm but rather with a Hill equation displaying a Hill coefficient of 2. The sensor, therefore,

displays a 9-fold dynamic range with a cooperative dose-response curve^{119, 120} ranging from 40 to 360 μM with a K_d value near 120 μM , which is 6-fold higher than the value obtained for the creatinine aptamer alone by ITC (e.g., 19 μM). This can be explained by the higher energetic binding cost required to displace the sigDNA. However, we are still looking for a potential hypothesis to explain the highly cooperative response of this sensor. Interestingly, a similar high cooperativity was observed on an uric acid aptamer-based sensor that also employed a strand-displacement strategy, but, unfortunately, no explanation was provided.⁷⁸ Future work exploring the role of the sigDNA lengths or the effect of varying ionic strength of cations (e.g., K^+ , Na^+ or Mg^{2+}) may reveal further insight into this behaviour.^{78, 121-124}

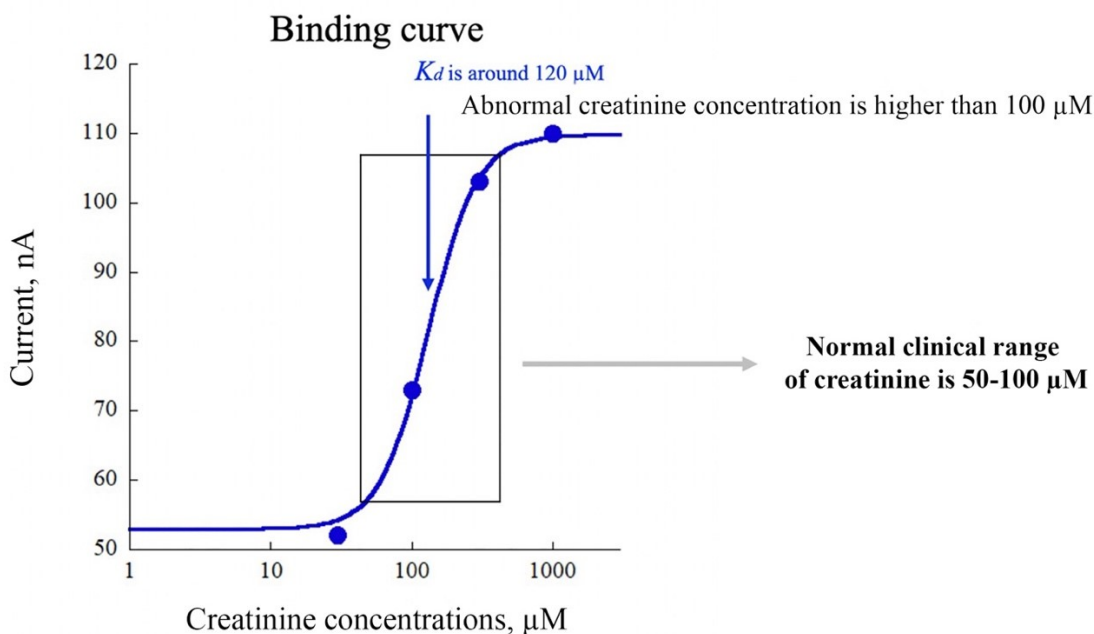


Figure 30. Binding curve and dynamic range of the electrochemical creatinine sensor. The data points are the average of triplicated measurements. The error bars, representing the standard deviations, are too small to be seen.

3.2.3.5. Detecting creatinine in serum

The new electrochemical sensing strategy demonstrates good performance in buffer. However, we also wanted to test its ability to detect creatinine in a complex medium such as serum. To determine whether the sensor works in serum, we first increased the working concentrations of sigDNA and aptamer in order to enhance the electrochemical signal, which is

typically lower in serum. Therefore, we used 200 nM of sigDNA and 600 nM of aptamer while keeping the optimal ratio of 1:3 between the sigDNA and the aptamer. We employed commercially available human serum of unknown creatinine concentration. For the negative control, we spiked the serum sample with creatinine deiminase, an enzyme that degrades creatinine into ammonia (*blue data*). We then evaluated the performance of the sensor by comparing the electrochemical signal obtained in serum (*pink data*), in serum with 1mM of added creatinine (*red data*) to serum containing the enzyme (*blue data*) (Fig. 31). The signal gain of an unknown creatinine concentration was 150 % compared to serum without creatinine (negative control with enzyme) after 5 min (*pink data*). Interestingly, the signal gain of detected 1 mM creatinine in serum was 400 % after 5 min but steadily decreasing with time (*red data*). This can be explained by DNA dissociation from the electrode surface; therefore, less sigDNA hybridizes to the capDNA and produces the electrochemical signal. Of note, the hybridization of the sigDNA also performs well in serum, as evidenced by a simple hybridization experiment performed in the absence of the aptamer (*green data*).

The preliminary results of the sensor displayed encouraging results in detecting the creatinine molecule in a complex matrix such as serum. However, there is still room for improvement, and more work and effort are required to determine the binding curve, the dynamic range and optimize the sensor's performance and reproducibility.

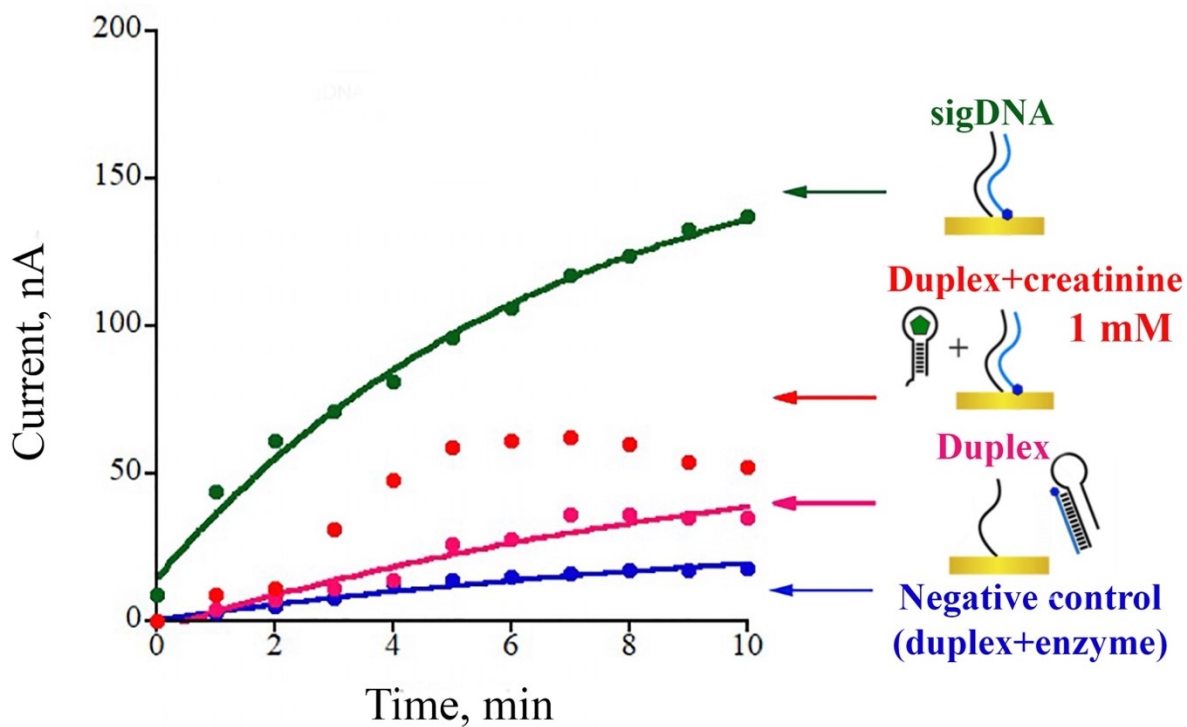
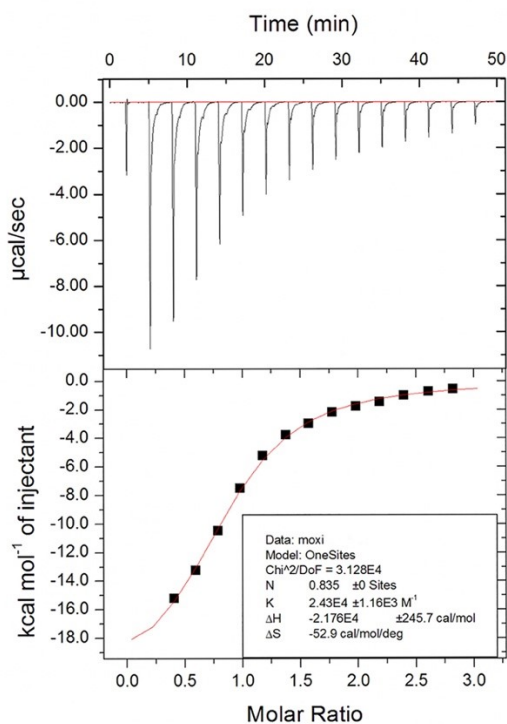


Figure 31. Creatinine detection directly in serum. The signal gain in the presence of an unknown creatinine concentration was 150%, and in 1 mM was 400% after 5min. The data points are the average of triplicated measurements. The error bars, representing the standard deviations, are too small to be seen.

3.3. Potential universality of the SELEX-based sensing strategy

To explore the universality of our proposed SELEX-based electrochemical sensing strategy, we have also adapted this signalling mechanism for the detection of moxifloxacin, an antibiotic used to treat bacterial infections.¹²⁵ To do so, we employed a moxifloxacin binding aptamer provided by the aptamer GROUP company that was selected by employing a similar SELEX strategy similar to the creatinine aptamer. Since no information was available concerning the affinity of this aptamer for moxifloxacin, we used ITC to determine its K_d (41 μM) (Fig. 34A). We then designed the DNA strands with specific labelling (see chapter 2, section 2.2) (e.g., capDNA and sigDNA) and tested the sensor directly in an electrochemical format. When employing 100 nM of sigDNA and 125 nM of aptamer, we obtained a signal gain of 150 % after 15 min in the presence of 100 μM moxifloxacin (Fig. 34B). Adding the preformed duplex sigDNA-moxifloxacin aptamer led to a low electrochemical signal (*pink data*). But, upon binding to moxifloxacin antibiotic, this duplex dissociated, releasing more sigDNA and producing a large electrochemical signal as expected (*blue data*). These results suggest that developing electrochemical aptamer-based sensors based on the selection procedure employed to select the aptamer provides an efficient, optimal way to develop novel electrochemical sensors.

A)



B)

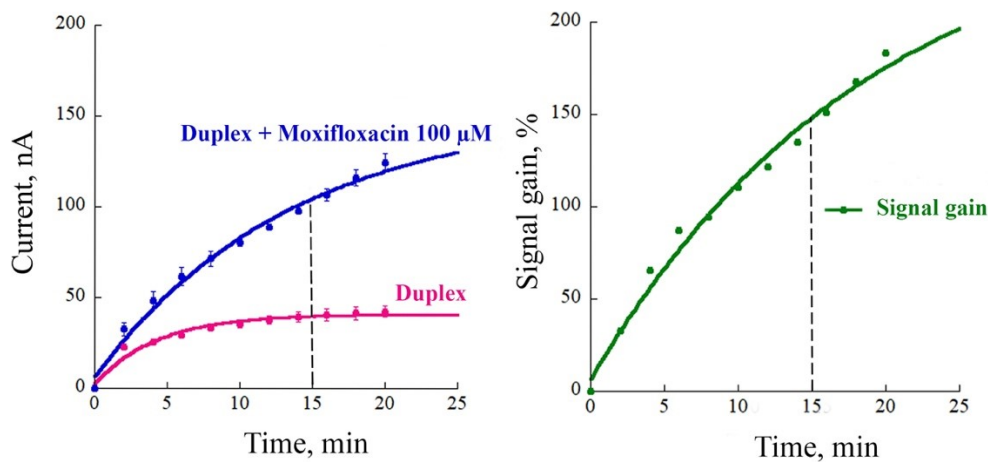


Figure 32. Developing a moxifloxacin sensor using a SELEX-based signalling mechanism. A) ITC characterization of the aptamer from Aptamer GROUP. B) Electrochemical detection of Moxifloxacin using a SELEX-based signalling mechanism. The signal gain was 150% after 15 min. The average data points are calculated from triplicated measurements. The error bars, representing the standard deviations, are too small to be seen.

Chapter 4 – Conclusions and Outlook

We have proposed and developed a novel strategy to engineer aptamer-based electrochemical biosensors by taking advantage of the capture-SELEX strategy by which aptamers are typically selected. More specifically, we developed two novel electrochemical biosensors: one for the detection of creatinine, an important marker of heart failure, and one to monitor Moxifloxacin, an important antibiotic.

The overall design strategy of this new class of sensors is relatively simple. We started by identifying and characterizing an aptamer that can bind to the specific marker of interest (in our case, creatinine, in order to monitor heart failure). Using ITC measurements, we determined the affinity between the aptamer and creatinine to make sure that the final sensor displays sufficient sensitivity for clinical application. In the case of creatinine and its aptamer, we found a dissociation constant, K_d , of 19 μM , which seems ideal for the typical clinical range of creatinine in blood (53 to 106 μM).¹¹ We also explored the relative selectivity of this aptamer by attempting to measure binding affinities between the creatinine-binding aptamer and another small amino-rich molecule present in blood (e.g., urea) and no binding was observed.

Prior to developing the new sensing architecture, we tried to adapt this aptamer to the well-known “one-component” and “three-component” electrochemical sensing mechanisms.^{63, 121, 126} However, the results were not encouraging, and these strategies did not work. Future research efforts could also be focused on the three-component assay to identify a more efficient binding location for the sigDNA in order to compete more successfully with the aptamer and the capDNA. Indeed, we tried only one location at the extremity of the aptamer, and maybe that location still enables creatinine binding, thus resulting in the sequestration of the sigDNA even in the presence of creatinine. Knowing that this aptamer is longer and contains stable secondary structures, we also explored three shorter versions of the aptamer (54 nt, 45nt and 36 nt) that may reduce the folding stability while facilitating the binding of the sigDNA. However, the shorter aptamer versions showed lower affinity or no affinity at all for creatinine, and we conclude that it is best to maintain the full aptamer length.

Since the SELEX-based signalling mechanism releases a short DNA strand, we first tested our designed strategy using a fluorescence assay often employed by the capture-SELEX research groups to characterize their selected aptamers.^{71-73, 78, 79, 81, 82, 127} This was realized by labelling the aptamer and the short strand (sigDNA) with a fluorophore and a quencher, respectively. In this first effort to detect creatinine by imitating the capture-based selection procedure, we successfully detected 0.5 mM of creatinine. Then we adapted this signalling mechanism into an electrochemical format by labelling the short DNA strand with a redox element (i.e., methylene blue) and observed a signal gain of 55 % after 15 min in the presence of 0.5 mM creatinine. Additional experiments were done to improve the signal gain of the sensor. For example, different ratios of sigDNA/aptamer ranging from 1:1 to 1:4 were explored. As expected, we found that having more aptamer decreased the background and improved the signal gain, but too much aptamer also requires higher creatinine concentrations to compete. We have also explored different lengths of the sigDNA to try to decrease the background signal and found that using the longer 14 nt sigDNA; the sensor achieved a signal gain of 75 % after 15 min (versus 55% for the 13 nt sigDNA).

Using this creatinine sensor, we then determined the dynamic range of our new biosensing strategy by spiking different concentrations of creatinine in a buffered solution. This preliminary binding curve suggests a cooperative dose-response relationship (a 9-fold dynamic range), enabling the accurate measurements of concentrations between 40 μ M and 360 μ M of creatinine. The higher estimated K_d value of the sensor, 120 μ M, is 10-fold higher than the one measured between creatinine and the aptamer using ITC (e.g., 19 μ M). However, the ITC experiment was performed in the absence of sigDNA, which likely reduces the energetic penalty related to the displacement of the sigDNA by the creatinine molecule.

Preliminary experiments on creatinine detection directly in serum displayed encouraging results. However, further experiments are needed to determine the dynamic range of this sensor in a complex medium, its reproducibility and performance optimization. If the selectivity and specificity of this sensor do not display satisfying performance, three other creatinine aptamers provided by our collaborator could also be adapted and tested.

Finally, we also explored the potential universality of our proposed signalling mechanism by developing a biosensor using the moxifloxacin aptamer. These results were encouraging because we obtained a large signal gain of 150 % after 15 min without any optimization. We hope that through the lens of a chemist, our contribution to the field of biosensors has shown how to design and adapt aptamer selection strategy (e.g., the capture-SELEX) in an electrochemical format.

In perspective, we believe that the next generation of electrochemical aptamer-based sensors may likely be developed by mimicking the selection strategy mechanism with which they have been selected. Nowadays, several companies are developing and improving aptamers, leading them to next-generation technologies.^{83, 128, 129} Perhaps in the near future, novel aptamer selection strategies could also be designed to select aptamers that are already optimized for a desired, preferred signalling mechanism. Therefore, the collaborative efforts of scientists from different fields should be considered to accelerate the advances in biosensors to detect heart failure markers and make the technology more affordable for patients.

We also predict that recent advances in the development and commercialization process of electrochemical DNA-based sensors are bringing us closer to the day when heart failure patients will be able to monitor themselves in the comfort of their home.

References

1. Cook, C.; Cole, G.; Asaris, P.; Jabbour, R.; Francis, D., The Annual Global Economic Burden of Heart Failure. *Heart* **2014**, *100*, A28-A29.
2. Benjamin, E. J.; Muntner, P.; Alonso, A.; Bittencourt, M. S.; Callaway, C. W.; Carson, A. P.; Chamberlain, A. M.; Chang, A. R.; Cheng, S.; Das, S. R.; Delling, F. N.; Djousse, L.; Elkind, M. S. V.; Ferguson, J. F.; Fornage, M.; Jordan, L. C.; Khan, S. S.; Kissela, B. M.; Knutson, K. L.; Kwan, T. W.; Lackland, D. T.; Lewis, T. T.; Lichtman, J. H.; Longenecker, C. T.; Loop, M. S.; Lutsey, P. L.; Martin, S. S.; Matsushita, K.; Moran, A. E.; Mussolino, M. E.; O'Flaherty, M.; Pandey, A.; Perak, A. M.; Rosamond, W. D.; Roth, G. A.; Sampson, U. K. A.; Satou, G. M.; Schroeder, E. B.; Shah, S. H.; Spartano, N. L.; Stokes, A.; Tirschwell, D. L.; Tsao, C. W.; Turakhia, M. P.; VanWagner, L. B.; Wilkins, J. T.; Wong, S. S.; Virani, S. S., Heart Disease and Stroke Statistics—2019 Update: A Report From the American Heart Association. *Circulation* **2019**, *139* (10), e56-e528.
3. Heart&Stroke, Heart failure in Canada: complex, incurable and on the rise. <https://www.heartandstroke.ca/what-we-do/media-centre/news-releases/heart-failure-in-canada-complex-incurable-and-on-the-rise> (accessed May 10th, 2022).
4. Khan, M. S.; Sreenivasan, J.; Lateef, N.; Abougergi, M. S.; Greene, S. J.; Ahmad, T.; Anker, S. D.; Fonarow, G. C.; Butler, J., Trends in 30- and 90-Day Readmission Rates for Heart Failure. *Circ Heart Fail* **2021**, *14* (4), e008335.
5. Rosano, G. M. C.; Seferović, P. M., Physiological monitoring in the complex multi-morbid heart failure patient - Introduction. *European Heart Journal Supplements* **2019**, *21* (Supplement_M), M1-M4.
6. Bui, A. L.; Fonarow, G. C., Home monitoring for heart failure management. *J Am Coll Cardiol* **2012**, *59* (2), 97-104.
7. Wang, J.; Tan, G. J.; Han, L. N.; Bai, Y. Y.; He, M.; Liu, H. B., Novel biomarkers for cardiovascular risk prediction. *J Geriatr Cardiol* **2017**, *14* (2), 135-150.
8. Metra, M.; Cotter, G.; Gheorghiade, M.; Dei Cas, L.; Voors, A. A., The role of the kidney in heart failure. *Eur Heart J* **2012**, *33* (17), 2135-42.

9. Kazory, A.; Ronco, C., Are We Barking Up the Wrong Tree? Rise in Serum Creatinine and Heart Failure. *Blood Purif* **2019**, *48* (3), 193-195.
10. Diagnostics Roche., Roche Diabetes Care.
https://diagnostics.roche.com/in/en_gb/about/about-roche-diabetes-care.html (accessed June 10th, 2022).
11. Walker, H. K.; Hall, W. D.; Hurst, J. W., *Clinical methods : the history, physical, and laboratory examinations*. 2d ed.; Butterworths: Boston, 1980; p xxiii, 1224, 15 p.
12. Wyss, M.; Kaddurah-Daouk, R., Creatine and creatinine metabolism. *Physiol Rev* **2000**, *80* (3), 1107-213.
13. Cánovas, R.; Cuartero, M.; Crespo, G. A., Modern creatinine (Bio)sensing: Challenges of point-of-care platforms. *Biosens Bioelectron* **2019**, *130*, 110-124.
14. Bonilla, D. A.; Kreider, R. B.; Stout, J. R.; Forero, D. A.; Kerksick, C. M.; Roberts, M. D.; Rawson, E. S., Metabolic Basis of Creatine in Health and Disease: A Bioinformatics-Assisted Review. *Nutrients* **2021**, *13* (4).
15. Chernecky, C. C.; Berger, B. J., *Laboratory tests and diagnostic procedures*. 3rd ed.; W.B. Saunders: Philadelphia, 2001; p xix, 1114 p.
16. Peake, M.; Whiting, M., Measurement of serum creatinine--current status and future goals. *Clin Biochem Rev* **2006**, *27* (4), 173-184.
17. Goldman, L.; Schafer, A. I., *Goldman-Cecil medicine*. 26th edition. ed.; Elsevier: Philadelphia, PA, 2020; p 2 volumes (xl, 1350, xl, 1351-2664 pages).
18. Lopez-Vilella, R.; Marques-Sule, E.; Sanchez-Lazaro, I.; Laymito Quispe, R.; Martinez Dolz, L.; Almenar Bonet, L., Creatinine and NT-ProBNP levels could predict the length of hospital stay of patients with decompensated heart failure. *Acta Cardiol* **2021**, 1-8.
19. Küme, T.; Sağlam, B.; Ergon, C.; Sisman, A. R., Evaluation and comparison of Abbott Jaffe and enzymatic creatinine methods: Could the old method meet the new requirements? *Journal of clinical laboratory analysis* **2018**, *32* (1), e22168.
20. Delanghe, J. R.; Speeckaert, M. M., Creatinine determination according to Jaffe-what does it stand for? *NDT Plus* **2011**, *4* (2), 83-86.

21. Debus, B.; Kirsanov, D.; Yaroshenko, I.; Sidorova, A.; Piven, A.; Legin, A., Two low-cost digital camera-based platforms for quantitative creatinine analysis in urine. *Analytica Chimica Acta* **2015**, *895*, 71-79.
22. Narimani, R.; Esmaeili, M.; Rasta, S. H.; Khosroshahi, H. T.; Mobed, A., Trend in creatinine determining methods: Conventional methods to molecular-based methods. *Analytical Science Advances* **2021**, *2* (5-6), 308-325.
23. Nova Biomedical, StatSensor and StatSensor Xpress Creatinine and eGFR Meters. <https://www.novabiomedical.com/statstrip-creatinine/> (accessed May 23th, 2022).
24. Abbott Global Point of Care, i-STAT 1, a handheld blood analyzer. <https://www.globalpointofcare.abbott/en/product-details/apoc/i-stat-system-us.html> (accessed May 24th, 2022).
25. Piccolo Xpress, chemistry analyzer, Piccolo Xpress. https://www.abaxis.com/piccolo-xpress?language_content_entity=en (accessed May 24th, 2022).
26. Siemens Healthineers, Health, S. epoc[®] Blood Analysis System. <https://www.siemens-healthineers.com/blood-gas/blood-gas-systems/epoc-blood-analysis-system> (accessed May 23th, 2022).
27. AdvaCare, StatSensor Creatinine Test strip 50/Ca. <https://advacaresupply.com/products/statsensor-creatinine-test-strip-50-ca?variant=31012087988287> (accessed July 28th, 2022).
28. NICE National Institute for Health and Care Excellence, i STAT CG4+ and CHEM8+ cartridges for point-of-care testing in the emergency department <https://www.nice.org.uk/advice/mib38/resources/i-stat-cg4-and-chem8-cartridges-for-pointofcare-testing-in-the-emergency-department-pdf-63499112313541/>(accessed July 25th, 2022).
29. LabX shop lab equipment, Abaxis Piccolo Xpress. <https://www.labx.com/product/abaxis-piccolo-xpress> (accessed July 28th, 2022).
30. Medex+ supply, Piccolo Xpress Basic Metabolic Panel Reagent Disc, 10/Box. <https://medexsupply.com/piccolo-xpress-basic-metabolic-panel-reagent-disc-10-box/> (accessed July 28th, 2022).

31. Fisher scientific part of Thermo Fisher Scientific, Siemens Healthineers Epoc™ BGEM Test Card with Creatinine and Cl-. <https://www.fishersci.com/shop/products/epoc-bgem-test-card-creatinine-cl/22347440> (accessed July 28th, 2022).
32. Cammann, K., Bio-sensors based on ion-selective electrodes. *Fresenius' Zeitschrift für analytische Chemie* **1977**, 287 (1), 1-9.
33. Thévenot, D. R.; Toth, K.; Durst, R. A.; Wilson, G. S., Electrochemical biosensors: recommended definitions and classification. *Biosens Bioelectron* **2001**, 16 (1-2), 121-31.
34. Bhalla, N.; Jolly, P.; Formisano, N.; Estrela, P., Introduction to biosensors. *Essays Biochem* **2016**, 60 (1), 1-8.
35. Kim, J.; Campbell, A. S.; de Avila, B. E. F.; Wang, J., Wearable biosensors for healthcare monitoring. *Nature Biotechnology* **2019**, 37 (4), 389-406.
36. Bhalla, N.; Jolly, P.; Formisano, N.; Estrela, P., Introduction to biosensors. *Essays Biochem* **2016**, 60 (1), 1-8.
37. Sethi, R. S., Transducer aspects of biosensors. *Biosensors and Bioelectronics* **1994**, 9 (3), 243-264.
38. IDTechEx Research reports, Biomedical Diagnostics at Point-of-Care 2019-2029: Technologies, Applications, Forecasts. <https://www.idtechex.com/en/research-report/biomedical-diagnostics-at-point-of-care-2019-2029-technologies-applications-forecasts/622> (accessed May 14th, 2022).
39. Higson, S.; Safari Books Online (Firm), Biosensors for medical applications. In *Woodhead Publishing series in biomaterials*, [Online] Woodhead Pub Ltd,: Oxford, 2012; pp. 1 online resource (xviii, 337 pages). <https://go.oreilly.com/yale-university/library/view/-/9781845699352/?ar> (accessed August 4th, 2022).
40. Clark, L. C., Jr.; Lyons, C., Electrode systems for continuous monitoring in cardiovascular surgery. *Ann N Y Acad Sci* **1962**, 102, 29-45.
41. Chard, T., Pregnancy tests: a review. *Hum Reprod* **1992**, 7 (5), 701-10.
42. Clarke, S. F.; Foster, J. R., A history of blood glucose meters and their role in self-monitoring of diabetes mellitus. *Br J Biomed Sci* **2012**, 69 (2), 83-93.

43. Ehrenkranz, J. R., Home and point-of-care pregnancy tests: a review of the technology. *Epidemiology* **2002**, *13 Suppl 3*, S15-8.
44. 1 First Response, OUR PREGNANCY TESTS. <https://firstresponsefertility.com/our-products> (accessed June 15th, 2022).
45. Campbell University -APHA Operation Diabetes, "Booklet: Blood Glucose Monitoring". <https://assets.campbell.edu/wp-content/uploads/sites/17/2021/02/Blood-Glucose-Monitoring.pdf> (accessed June 15th, 2022).
46. Gibson, T. D., Biosensors: The stability problem. *Analisis* **1999**, *27 (7)*, 630-638.
47. Sassolas, A.; Blum, L. J.; Leca-Bouvier, B. D., Immobilization strategies to develop enzymatic biosensors. *Biotechnology Advances* **2012**, *30 (3)*, 489-511.
48. Witkowska Nery, E.; Kundys, M.; Jeleń, P. S.; Jönsson-Niedziółka, M., Electrochemical Glucose Sensing: Is There Still Room for Improvement? *Analytical Chemistry* **2016**, *88 (23)*, 11271-11282.
49. Peeling, R. W.; Holmes, K. K.; Mabey, D.; Ronald, A., Rapid tests for sexually transmitted infections (STIs): the way forward. *Sexually Transmitted Infections* **2006**, *82 (suppl 5)*, v1-v6.
50. Giljohann, D. A.; Mirkin, C. A., Drivers of biodiagnostic development. *Nature* **2009**, *462 (7272)*, 461-464.
51. Ronkainen, N. J.; Halsall, H. B.; Heineman, W. R., Electrochemical biosensors. *Chem Soc Rev* **2010**, *39 (5)*, 1747-63.
52. Drummond, T. G.; Hill, M. G.; Barton, J. K., Electrochemical DNA sensors. *Nat Biotechnol* **2003**, *21 (10)*, 1192-9.
53. Odenthal, K. J.; Gooding, J. J., An introduction to electrochemical DNA biosensors. *Analyst* **2007**, *132 (7)*, 603-10.
54. Fan, C.; Plaxco, K. W.; Heeger, A. J., Electrochemical interrogation of conformational changes as a reagentless method for the sequence-specific detection of DNA. *Proceedings of the National Academy of Sciences* **2003**, *100 (16)*, 9134.
55. Wu, Y.; Lai, R. Y., Tunable Signal-Off and Signal-On Electrochemical Cisplatin Sensor. *Analytical Chemistry* **2017**, *89 (18)*, 9984-9989.

56. Dong, Y., *Aptamers for Analytical Applications: Affinity Acquisition and Method Design*. WILEY: 2019.
57. Lakhin, A. V.; Tarantul, V. Z.; Gening, L. V., Aptamers: problems, solutions and prospects. *Acta Naturae* **2013**, 5 (4), 34-43.
58. Arroyo-Curras, N.; Dauphin-Ducharme, P.; Scida, K.; Chavez, J. L., From the beaker to the body: translational challenges for electrochemical, aptamer-based sensors. *Analytical Methods* **2020**, 12 (10), 1288-1310.
59. Ellington, A. D.; Szostak, J. W., In vitro selection of RNA molecules that bind specific ligands. *Nature* **1990**, 346 (6287), 818-822.
60. Tuerk, C.; Gold, L., Systematic evolution of ligands by exponential enrichment: RNA ligands to bacteriophage T4 DNA polymerase. *Science* **1990**, 249 (4968), 505.
61. Introduction of SELEX and Important SELEX Variants. In *Aptamers for Analytical Applications*, 2018; pp 1-25.
62. Zhuo, Z.; Yu, Y.; Wang, M.; Li, J.; Zhang, Z.; Liu, J.; Wu, X.; Lu, A.; Zhang, G.; Zhang, B., Recent Advances in SELEX Technology and Aptamer Applications in Biomedicine. *Int J Mol Sci* **2017**, 18 (10).
63. Xiao, Y.; Lubin, A. A.; Heeger, A. J.; Plaxco, K. W., Label-free electronic detection of thrombin in blood serum by using an aptamer-based sensor. *Angew Chem Int Ed Engl* **2005**, 44 (34), 5456-9.
64. Baker, B. R.; Lai, R. Y.; Wood, M. S.; Doctor, E. H.; Heeger, A. J.; Plaxco, K. W., An Electronic, Aptamer-Based Small-Molecule Sensor for the Rapid, Label-Free Detection of Cocaine in Adulterated Samples and Biological Fluids. *Journal of the American Chemical Society* **2006**, 128 (10), 3138-3139.
65. White, R. J.; Phares, N.; Lubin, A. A.; Xiao, Y.; Plaxco, K. W., Optimization of Electrochemical Aptamer-Based Sensors via Optimization of Probe Packing Density and Surface Chemistry. *Langmuir* **2008**, 24 (18), 10513-10518.
66. Zhu, G. *Novel universal electrochemical DNA-based signaling mechanisms for molecular detection in a drop of blood*. Ph.D. Thesis, Université de Montréal, **2022**.

67. Feagin, T. A.; Maganzini, N.; Soh, H. T., Strategies for Creating Structure-Switching Aptamers. *ACS Sensors* **2018**, *3* (9), 1611-1615.
68. Komarova, N.; Kuznetsov, A., Inside the Black Box: What Makes SELEX Better? *Molecules* **2019**, *24* (19).
69. Li, H.-H.; Wen, C.-Y.; Hong, C.-Y.; Lai, J.-C., Evaluation of aptamer specificity with or without primers using clinical samples for C-reactive protein by magnetic-assisted rapid aptamer selection. *RSC Advances* **2017**, *7* (68), 42856-42865.
70. Yang, K. A.; Pei, R.; Stojanovic, M. N., In vitro selection and amplification protocols for isolation of aptameric sensors for small molecules. *Methods* **2016**, *106*, 58-65.
71. Stojanovic, M. N.; de Prada, P.; Landry, D. W., Aptamer-Based Folding Fluorescent Sensor for Cocaine. *Journal of the American Chemical Society* **2001**, *123* (21), 4928-4931.
72. Lyu, C.; Khan, I. M.; Wang, Z. P., Capture-SELEX for aptamer selection: A short review. *Talanta* **2021**, 229.
73. Stoltenburg, R.; Nikolaus, N.; Strehlitz, B., Capture-SELEX: Selection of DNA Aptamers for Aminoglycoside Antibiotics. *J Anal Methods Chem* **2012**, 2012.
74. McKeague, M.; Derosa, M. C., Challenges and opportunities for small molecule aptamer development. *J Nucleic Acids* **2012**, 2012, 748913.
75. Ruscito, A.; DeRosa, M. C., Small-Molecule Binding Aptamers: Selection Strategies, Characterization, and Applications. *Front Chem* **2016**, 4.
76. Stoltenburg, R.; Reinemann, C.; Strehlitz, B., FluMag-SELEX as an advantageous method for DNA aptamer selection. *Analytical and Bioanalytical Chemistry* **2005**, *383* (1), 83-91.
77. Tian, H. L.; Duan, N.; Wu, S. J.; Wang, Z. P., Selection and application of ssDNA aptamers against spermine based on Capture-SELEX. *Analytica Chimica Acta* **2019**, *1081*, 168-175.
78. Liu, Y.; Liu, J., Selection of DNA Aptamers for Sensing Uric Acid in Simulated Tears. *Analysis & Sensing* **2022**, *n/a* (n/a), e202200038.
79. Nutiu, R.; Li, Y., In Vitro Selection of Structure-Switching Signaling Aptamers. *Angewandte Chemie International Edition* **2005**, *44* (7), 1061-1065.
80. Morse, D. P., Direct selection of RNA beacon aptamers. *Biochem Biophys Res Commun* **2007**, *359* (1), 94-101.

81. Qiao, Q. Q.; Guo, X. D.; Wen, F.; Chen, L.; Xu, Q. B.; Zheng, N.; Cheng, J. B.; Xue, X. H.; Wang, J. Q., Aptamer-Based Fluorescence Quenching Approach for Detection of Aflatoxin M-1 in Milk. *Front Chem* **2021**, *9*.
82. Nutiu, R.; Li, Y. F., Structure-switching signaling aptamers: Fluorescent DNA probes for drug discovery. *Abstr Pap Am Chem S* **2005**, 229, U118-U118.
83. aptamer?, A. G. W. i. a., **2020**.
84. Zuker, M., Mfold web server for nucleic acid folding and hybridization prediction. *Nucleic Acids Research* **2003**, *31* (13), 3406-3415.
85. IDT Integrated DNA Technologies, OligoAnalyzer tool. <https://www.idtdna.com/pages/tools/oligoanalyzer?returnurl=%2Fcalc%2Falyzer> (accessed May 5th, 2022).
86. Johnson, S. S. a. P. E., Isothermal titration calorimetry studies of aptamer-small molecule interactions: practicalities and pitfalls. *Aptamers* **2018**, *2*, 45-51.
87. GE Healthcare Life Sciences, "Getting Started Booklet: Isothermal Titration Calorimeter Introduction to iTC200". https://1stdirectory.co.uk/assets/files_comp/fc1d65ee-6c98-49c8-bfae-49fb26b9f955.pdf (accessed June 13th, 2022).
88. Song, C.; Zhang, S.; Huang, H., Choosing a suitable method for the identification of replication origins in microbial genomes. *Front Microbiol* **2015**, *6*, 1049.
89. Harvard Medical School system, "Manual: MicroCal iTC200 system User Manual". <https://cmi.hms.harvard.edu/files/cmi/files/microcal-itc200-system-user-manual.pdf> (accessed June 11th, 2022).
90. Herne, T. M.; Tarlov, M. J., Characterization of DNA probes immobilized on gold surfaces. *Journal of the American Chemical Society* **1997**, *119* (38), 8916-8920.
91. Lao, R.; Song, S.; Wu, H.; Wang, L.; Zhang, Z.; He, L.; Fan, C., Electrochemical Interrogation of DNA Monolayers on Gold Surfaces. *Analytical Chemistry* **2005**, *77* (19), 6475-6480.
92. Rashid, J. I. A.; Yusof, N. A., The strategies of DNA immobilization and hybridization detection mechanism in the construction of electrochemical DNA sensor: A review. *Sensing and Bio-Sensing Research* **2017**, *16*, 19-31.

93. Xiao, Y.; Lai, R. Y.; Plaxco, K. W., Preparation of electrode-immobilized, redox-modified oligonucleotides for electrochemical DNA and aptamer-based sensing. *Nat Protoc* **2007**, *2* (11), 2875-80.
94. Conguctive Technologies, Phase Zero Sensors Sell Sheet. <https://www.conductivetech.com/products/phase-zero-sensors/> (accessed May 24th, 2022).
95. Wang, J., *Analytical electrochemistry*. 3rd ed.; Wiley-VCH: Hoboken, N.J., 2006; p xvi, 250 p.
96. Teles, F. R. R.; Fonseca, L. P., Trends in DNA biosensors. *Talanta* **2008**, *77* (2), 606-623.
97. Keighley, S. D.; Li, P.; Estrela, P.; Migliorato, P., Optimization of DNA immobilization on gold electrodes for label-free detection by electrochemical impedance spectroscopy. *Biosens Bioelectron* **2008**, *23* (8), 1291-7.
98. Bard, A. J.; Faulkner, L. R., *Electrochemical methods : fundamentals and applications*. 2nd ed.; Wiley: New York, 2001; p xxi, 833 p.
99. Barsan, M. M.; Pinto, E. M.; Brett, C. M., Methylene blue and neutral red electropolymerisation on AuQCM and on modified AuQCM electrodes: an electrochemical and gravimetric study. *Phys Chem Chem Phys* **2011**, *13* (12), 5462-71.
100. Princeton Applied Research, "Brochure": Application Note S-7 Square Wave Voltammetry. https://www.ameteki.com/-/media/ameteki/download_links/documentations/library/princetonappliedresearch/application_note_s-7.pdf?revision=b24dbed0-321b-47a9-a940-97f04e047d5b (accessed May 26th, 2022).
101. Mahshid, S. S.; Ricci, F.; Kelley, S. O.; Vallee-Belisle, A., Electrochemical DNA-Based Immunoassay That Employs Steric Hindrance To Detect Small Molecules Directly in Whole Blood. *Acs Sensors* **2017**, *2* (6), 718-723.
102. Harris, D. C., *Quantitative chemical analysis*. 6th ed.; W.H. Freeman and Co.: New York, 2003.
103. Zakalskiy, A.; Stasyuk, N.; Gonchar, M., Creatinine Deiminase: Characterization, Using in Enzymatic Creatinine Assay, and Production of the Enzyme. *Curr Protein Pept Sc* **2019**, *20* (5), 465-470.

104. Grabowska, I.; Sharma, N.; Vasilescu, A.; Iancu, M.; Badea, G.; Boukherroub, R.; Ogale, S.; Szunerits, S., Electrochemical Aptamer-Based Biosensors for the Detection of Cardiac Biomarkers. *ACS Omega* **2018**, *3* (9), 12010-12018.
105. Idili, A.; Gerson, J.; Parolo, C.; Kippin, T.; Plaxco, K. W., An electrochemical aptamer-based sensor for the rapid and convenient measurement of L-tryptophan. *Anal Bioanal Chem* **2019**, *411* (19), 4629-4635.
106. Zuo, X.; Song, S.; Zhang, J.; Pan, D.; Wang, L.; Fan, C., A Target-Responsive Electrochemical Aptamer Switch (TREAS) for Reagentless Detection of Nanomolar ATP. *Journal of the American Chemical Society* **2007**, *129* (5), 1042-1043.
107. Asai, K.; Yamamoto, T.; Nagashima, S.; Ogata, G.; Hibino, H.; Einaga, Y., An electrochemical aptamer-based sensor prepared by utilizing the strong interaction between a DNA aptamer and diamond. *Analyst* **2020**, *145* (2), 544-549.
108. Ku, T. H.; Zhang, T.; Luo, H.; Yen, T. M.; Chen, P. W.; Han, Y.; Lo, Y. H., Nucleic Acid Aptamers: An Emerging Tool for Biotechnology and Biomedical Sensing. *Sensors (Basel)* **2015**, *15* (7), 16281-313.
109. Lu, Y.; Zhu, N. N.; Yu, P.; Mao, L. Q., Aptamer-based electrochemical sensors that are not based on the target binding-induced conformational change of aptamers. *Analyst* **2008**, *133* (9), 1256-1260.
110. Centi, S.; Tombelli, S.; Minunni, M.; Mascini, M., Aptamer-based detection of plasma proteins by an electrochemical assay coupled to magnetic beads. *Analytical Chemistry* **2007**, *79* (4), 1466-1473.
111. Mir, M.; Vreeke, M.; Katakis, L., Different strategies to develop an electrochemical thrombin aptasensor. *Electrochem Commun* **2006**, *8* (3), 505-511.
112. Ikebukuro, K.; Kiyohara, C.; Sode, K., Electrochemical detection of protein using a double aptamer sandwich. *Analytical Letters* **2004**, *37* (14), 2901-2909.
113. Zhu, C. X.; Liu, M. Y.; Li, X. Y.; Zhang, X. H.; Chen, J. H., A new electrochemical aptasensor for sensitive assay of a protein based on the dual- signaling electrochemical ratiometric method and DNA walker strategy. *Chem Commun* **2018**, *54* (73), 10359-10362.

114. Harroun, S. G.; Prévost-Tremblay, C.; Lauzon, D.; Desrosiers, A.; Wang, X.; Pedro, L.; Vallée-Bélisle, A., Programmable DNA switches and their applications. *Nanoscale* **2018**, *10* (10), 4607-4641.
115. Marras, S. A.; Kramer, F. R.; Tyagi, S., Efficiencies of fluorescence resonance energy transfer and contact-mediated quenching in oligonucleotide probes. *Nucleic Acids Res* **2002**, *30* (21), e122.
116. Vallée-Bélisle, A.; Ricci, F.; Plaxco, K. W., Thermodynamic basis for the optimization of binding-induced biomolecular switches and structure-switching biosensors. *Proceedings of the National Academy of Sciences* **2009**, *106* (33), 13802-13807.
117. Ricci, F.; Vallee-Belisle, A.; Porchetta, A.; Plaxco, K. W., Rational design of allosteric inhibitors and activators using the population-shift model: in vitro validation and application to an artificial biosensor. *J Am Chem Soc* **2012**, *134* (37), 15177-80.
118. Labcompare laboratory equipment <https://www.labcompare.com/Clinical-Diagnostics/5104-Creatinine-Analyzer/>(accessed November 10th, 2022).
119. Simon, A. J.; Vallee-Belisle, A.; Ricci, F.; Watkins, H. M.; Plaxco, K. W., Using the population-shift mechanism to rationally introduce "Hill-type" cooperativity into a normally non-cooperative receptor. *Angew Chem Int Ed Engl* **2014**, *53* (36), 9471-5.
120. Ricci, F.; Vallee-Belisle, A.; Plaxco, K. W., High-precision, in vitro validation of the sequestration mechanism for generating ultrasensitive dose-response curves in regulatory networks. *PLoS Comput Biol* **2011**, *7* (10), e1002171.
121. A.Vallee-Belisle, G. Zhu. U.S. Patent App. 17/057,202, 2021.
122. Nutiu, R.; Li, Y. F., Structure-switching signaling aptamers. *Journal of the American Chemical Society* **2003**, *125* (16), 4771-4778.
123. Kang, D.; Vallee-Belisle, A.; Porchetta, A.; Plaxco, K. W.; Ricci, F., Re-engineering electrochemical biosensors to narrow or extend their useful dynamic range. *Angew Chem Int Ed Engl* **2012**, *51* (27), 6717-21.
124. Li, S.; Li, C.; Wang, Y.; Li, H.; Xia, F., Re-engineering Electrochemical Aptamer-Based Biosensors to Tune Their Useful Dynamic Range via Distal-Site Mutation and Allosteric Inhibition. *Anal Chem* **2020**, *92* (19), 13427-13433.

125. Keating, G. M.; Scott, L. J., Moxifloxacin: a review of its use in the management of bacterial infections. *Drugs* **2004**, *64* (20), 2347-77.
126. Baker, B. R.; Lai, R. Y.; Wood, M. S.; Doctor, E. H.; Heeger, A. J.; Plaxco, K. W., An electronic, aptamer-based small-molecule sensor for the rapid, label-free detection of cocaine in adulterated samples and biological fluids. *J Am Chem Soc* **2006**, *128* (10), 3138-9.
127. Nutiu, R.; Li, Y. F., In vitro selection of structure-switching signaling aptamers. *Angew Chem Int Edit* **2005**, *44* (7), 1061-1065.
128. Raptamer Discovery Group. <https://raptamer.com/> (accessed November 10th, 2022).
129. Aptagen Company <https://www.aptagen.com/what-are-aptamers/> (accessed November 10th, 2022).